Single-dose immunization with a chimpanzee adenovirus-based vaccine induces sustained and protective immunity against SARS-CoV-2 infection

Linqi Zhang (zhanglinqi@tsinghua.edu.cn)
Tsinghua University https://orcid.org/0000-0003-4931-509X

Mingxi Li
Tsinghua University

Jingao Guo
University of Chinese Academy of Sciences, Chinese Academy of Sciences

Shuaiyao Lu
Chinese Academy of Medical Sciences & Peking Union Medical College https://orcid.org/0000-0003-1675-9735

Runhong Zhou
University of Hong Kong

Hongyang Shi
University of Chinese Academy of Sciences, Chinese Academy of Sciences

Xuangling Shi
Tsinghua University

Lin Cheng
Shenzhen Third People's Hospital

Qingtai Liang
Tsinghua University

Hongqi Liu
Institute of Medical Biology,Chinese Academy of Medical Sciences. https://orcid.org/0000-0002-8564-0247

Pui Wang
University of Hong Kong

Nan Wang
Tsinghua University

Yifeng Wang
Tsinghua University

Lili Fu
Tsinghua University

Man Xing

Tianjin Medical University

Bin Ju

Shenzhen Third People's Hospital, Southern University of Science and Technology

Li Liu

University of Hong Kong https://orcid.org/0000-0003-2566-7357

Siu-Ying Lau

University of Hong Kong

Wenxu Jia

Tsinghua University

Xin Tong

Walvax Biotechnology Co., Ltd.

Lin Yuan

Walvax Biotechnology Co., Ltd.

Yong Guo

Tsinghua University

Hai Qi

Tsinghua University

Qi Zhang

Tsinghua University

Zhen Huang

Walvax Biotechnology Co., Ltd.

Honglin Chen

University of Hong Kong https://orcid.org/0000-0001-5108-8338

Zheng Zhang

Institute for Hepatology, National Clinical Research Center for Infectious Disease, Shenzhen Third People&#x2019 https://orcid.org/0000-0002-3544-1389

Zhiwei Chen

the University of Hong Kong https://orcid.org/0000-0002-4511-2888

Xiaozhong Peng

Chinese Academy of Medical Sciences & Peking Union Medical College

Dongming Zhou

Tianjin Medical University https://orcid.org/0000-0002-5989-7591

Ruoke Wang

Tsinghua University https://orcid.org/0000-0002-8040-7913

Article

Keywords: SARS-CoV-2, adenovirus vaccine, ChAdTS-S, immune responses, ChAdTS-RBD, ChAdTS-RBD

Posted Date: February 23rd, 2021

DOI: https://doi.org/10.21203/rs.3.rs-155550/v1

Single-dose immunization with a chimpanzee adenovirus-based vaccine induces sustained and protective immunity against SARS-CoV-2 infection

Mingxi Li[1,21], Jingao Guo[2,3,21], Shuaiyao Lu[4,5,21], Runhong Zhou[6,7,21], Hongyang Shi[2,3,21], Xuanling Shi[1,21], Lin Cheng[8,9], Qingtai Liang[1], Hongqi Liu[4], Pui Wang[7], Nan Wang[10], Yifeng Wang[11,12,13], Lili Fu[1], Man Xing[14], Ruoke Wang[1], Bin Ju[8,9], Li Liu[6,7], Siu-Ying Lau[7], Wenxu Jia[1,15], Xin Tong[16], Lin Yuan[16], Yong Guo[10], Hai Qi[11,12,13,17,18,19], Qi Zhang[1], Zhen Huang[16], Honglin Chen[7], Zheng Zhang[8,9], Zhiwei Chen[6,7]*, Xiaozhong Peng[4,5]*, Dongming Zhou[14,20]*, Linqi Zhang[1]*

[1]Comprehensive AIDS Research Center, Beijing Advanced Innovation Center for Structural Biology, School of Medicine and Vanke School of Public Health, Tsinghua University, 100084, Beijing, China.

[2]University of Chinese Academy of Sciences, 100049, Beijing, China.

[3]Chinese Academy of Sciences, 200031, Shanghai, China.

[4]National Kunming High-level Biosafety Primate Research Center, Institute of Medical Biology, Chinese Academy of Medical Sciences and Peking Union Medical College, Kunming, Yunnan Province, China.

[5]State Key Laboratory of Medical Molecular Biology, Department of Molecular Biology and Biochemistry, Institute of Basic Medical Sciences, Medical Primate Research Center, Neuroscience Center, Chinese Academy of Medical Sciences, School of Basic Medicine, Peking Union Medical College, Beijing, China.

[6]AIDS Institute, Li Ka Shing Faculty of Medicine, The University of Hong Kong, Hong Kong Special Administrative Region (SAR), China.

[7]State Key Laboratory for Emerging Infectious Diseases, Department of Microbiology, Li Ka Shing Faculty of Medicine, The University of Hong Kong, Hong Kong SAR, China.

[8]Institute for Hepatology, National Clinical Research Center for Infectious Disease, Shenzhen Third People's Hospital, 518112, Shenzhen, Guangdong Province, China.

[9]The Second Affiliated Hospital, School of Medicine, Southern University of Science and Technology, 518055, Shenzhen, Guangdong Province, China.

[10]Department of Biomedical Engineering, School of Medicine, Tsinghua University, 100084, Beijing, China.

[11]Tsinghua-Peking Center for Life Sciences, Tsinghua University, 100084, Beijing, China.

[12]Laboratory of Dynamic Immunobiology, Institute for Immunology, Tsinghua University, 100084, Beijing, China.

[13]Department of Basic Medical Sciences, School of Medicine, Tsinghua University, 100084, Beijing, China.

[14]Department of Pathogen Biology, School of Basic Medical Sciences, Tianjin Medical University, 300070, Tianjin, China.

[15]Teaching center for writing and communication, Tsinghua University, 100084, Beijing, China.

[16]Walvax Biotechnology Co., Ltd., Yunnan, China

[17]School of Life Sciences, Tsinghua University, 100084, Beijing, China

[18]Beijing Key Laboratory for Immunological Research on Chronic Diseases, Tsinghua University, 100084, Beijing, China.

[19]Beijing Frontier Research Center for Biological Structure, Tsinghua University, 100084, Beijing, China.

[20]Shanghai Public Health Clinical Center, Fudan University, 201508, Shanghai, China.

[21]These authors contributed equally: Mingxi Li, Jingao Guo, Shuaiyao Lu, Runhong Zhou, Hongyang Shi, Xuanling Shi.

e-mail: zchenai@hku.hk, pengxiaozhong@pumc.edu.cn, zhoudongming@tmu.edu.cn, zhanglinqi@tsinghua.edu.cn.

Abstract

The development of an effective vaccine against SARS-CoV-2, the causative agent of pandemic coronavirus disease-2019 (COVID-19), is a global priority. Here, we present three chimpanzee adenovirus vaccines that express either the full-length spike (ChAdTS-S), or receptor-binding domain (RBD) with two different signal sequences (ChAdTS-RBD and ChAdTS-RBDs). Single-dose intranasal or intramuscular immunization induced robust and sustained neutralizing antibody responses in BALB/c mice, with ChAdTS-S being superior to ChAdTS-RBD and ChAdTS-RBDs. Intranasal immunization appeared to induce a predominately Th2-based response whereas intramuscular administration resulted in a predominately Th1 response. The neutralizing activity against several circulating SARS-CoV-2 variants remained unaffected for mice serum but reduced for rhesus macaque serum. Importantly, immunization with ChAdTS-S via either route induced protective immunity against high-dose challenge with live SARS-CoV-2 in rhesus macaques. Vaccinated macaques demonstrated dramatic decreases in viral RNA in the lungs and nasal swabs, as well as reduced lung pathology compared to the control animals. Similar protective effects were also found in a golden Syrian hamster model of SARS-CoV-2 infection. Taken together, these results confirm that ChAdTS-S can induce protective immune responses in experimental animals, meriting further development toward a human vaccine against SARS-CoV-2.

Introduction

The rapid and global spread of severe acute respiratory syndrome coronavirus 2 (SARS-CoV-2), the causative agent of coronavirus disease-2019 (COVID-19), calls for urgent development of safe, effective and equitably accessible vaccines. Since the release of the genome sequence of SARS-CoV-2 in early January of 2020, scientists and industrial partners around the world have been working tirelessly to develop various vaccines based on traditional and innovative platforms, each of which is expected to result in different safety and efficacy profiles in humans. For example, the mRNA vaccines developed by Pfizer/BioNtech and Moderna have recently been approved for emergency use by several regulatory agencies. The entire pipeline relies on innovative technologies for both antigen design and gene expression, which offer unprecedented speed and flexibility[1-3]. However, the long-term safety, efficacy and durability of protection require further characterization. The rare-serotype adenovirus-based vaccines, being developed by AstraZeneca/Oxford University (ChAdOX1) and Johnson & Johnson (Ad26), have also incorporated novel features for antigen- and vector optimization. Given their prior experience in similar vector-based vaccines against Middle East Respiratory Syndrome Coronavirus (MERS-CoV) and human immunodeficiency virus type I (HIV-1)[4,5], this strategy is likely to be superior in large-scale manufacturing, distribution and administration of vaccines, which may practically translate into larger accessibility and greater protection at the population level. Furthermore, killed vaccines have also been developed, demonstrating impressive safety and efficacy profiles in phase III human trials around the world. This classic form of vaccine has a proven record of success in inducing protective immunity in humans against various viral pathogens, although potential risks exist when manufacturing and handling industrial amounts of live infectious particles[6]. Additional vaccine platforms,

based on DNA, recombinant proteins, or novel viral vectors, are also being developed[7-10].

The reported vaccine candidates incorporate either the full-length spike (S) protein of SARS-CoV-2 or only its receptor-binding domain (RBD) as the immunogen, since the RBD of S plays critical roles in mediating viral entry[11-13] and inducing a protective antibody response in infected individuals as well as experimental animals[14-18]. Similar to other coronaviruses, the S protein of SARS-CoV-2 consists of a globular S1 domain, an N-terminal region, a membrane-proximal S2 domain, and a transmembrane domain[11]. The RBD, which is located within the S1 domain, determines the host range and cellular tropism, while the S2 domain mediates membrane fusion[11]. SARS-CoV-2 infects airway epithelial cells via an interaction of the RBD with the cellular receptor angiotensin-converting enzyme 2 (ACE2) [19]. We and others recently resolved the crystal structure of the SARS-CoV-2 RBD bound to ACE2, which revealed that the overall ACE2-binding mode is nearly identical to that of the SARS-CoV RBD, which also utilizes ACE2 as the cellular receptor[13,19-21]. This suggests that agents capable of disrupting this binding interaction could serve as candidates to block the entry of SARS-CoV-2 into target cells. Indeed, both polyclonal and monoclonal antibodies directed against the RBD and the S protein in general have been shown to inhibit SARS-CoV-2 infection[14,18,22]. A large number of neutralizing monoclonal antibodies that target the RBD of SARS-CoV-2 also provide protection against infection in experimental animal models[15,22-25]. Crystal structure analysis of these neutralizing antibodies revealed their spatial overlaps and competition with ACE2 for binding to RBD, thereby disrupting the viral cell-entry process[14,22,25,26]. Importantly, the reported vaccines that are being investigated or have been approved for emergency use target either the S protein or the RBD, and have shown to elicit protective immunity in various

126 animal models and humans, reinforcing the scientific rationale to incorporate S or the
127 RBD as vaccine immunogens.
128 After weighing the advantages and disadvantages of various strategies, we sought to
129 develop a novel SARS-CoV-2 vaccine based on the less commonly used rare-
130 serotype adenovirus vector ChAdTS, a derivative of replication-defective chimpanzee
131 adenovirus type 68 (AdC68). Apart from low pre-existing immunity in humans, this
132 vector was demonstrated to induce strong and long-lasting immunity against various
133 viral antigens in experimental animals[27-29]. For example, the parental AdC68 vector
134 was used by our group to develop a vaccine candidate expressing the full-length
135 MERS-CoV S glycoprotein. Single-dose intranasal administration of this vaccine
136 completely protected human DPP4 knock-in mice from lethal MERS-CoV challenge.
137 Passive transfer of immune sera also conferred a survival advantage in lethal
138 challenge mouse models[27]. This is in great contrast to the immunity induced by other
139 candidate vaccines, for which immunogenicity is short-lived and multiple rounds of
140 immunization are required to induce detectable levels of neutralizing antibodies or to
141 confer protection against viral challenge[1,30]. Furthermore, recombinant vaccines
142 based on AdC68 and other rare serotype chimpanzee adenoviral vectors, such as
143 ChAd63 and ChAd3, have recently been engineered to express various antigens, with
144 some demonstrating impressive safety and immunogenicity profiles in clinical
145 studies[31-35]. These unique features and our prior experience in handling the
146 chimpanzee adenovirus vectors provided a critical foundation and rationale for the
147 development of a SARS-CoV-2 vaccine based on ChAdTS.
148 The immunogen was either the full-length spike (ChAdTS-S), the receptor-binding
149 domain with the cognate signal sequence (ChAdTS-RBD), or the RBD with the
150 secretory signal sequence from mouse IgG (ChAdTS-RBDs). Single-dose intranasal

or intramuscular immunization with these three vaccine candidates induced a robust and sustained neutralizing antibody response in BALB/c mice, with ChAdTS-S being superior to ChAdTS-RBD and ChAdTS-RBDs. ChAdTS-S immunization through the IN route induced a predominately Th2-biased response, while the IM route resulted in a predominately Th1 response. Such biased immune responses are further supported by the analysis of T-cell responses in immunized animals. Importantly, either administration route was able to induce robust and protective immunity against a live-virus challenge in both golden Syrian hamsters and rhesus macaques, supporting the further development of ChAdTS-S into a clinical vaccine against SARS-CoV-2 infection in humans.

Results

Generation and characterization of recombinant ChAdTS vaccines expressing the spike and RBD of SARS-CoV-2 We generated three recombinant ChAdTS vaccines, expressing either the full-length S protein with the original signal peptide (ChAdTS-S), the RBD with the original signal peptide of the S protein (ChAdTS-RBD), or the RBD with a secretory signal peptide (ChAdTS-RBDs) (Fig. 1a). The coding sequences of S or RBD were inserted into the E1 region of the ChAdTS vector under the control of the CMV promoter and terminated with a bovine growth hormone (BGH) polyadenylation signal sequence. HEK293T cells infected with ChAdTS-S, ChAdTS-RBD, ChAdTS-RBDs showed the desired expression of S or RBD according to both western blot (Fig. 1b) and flow cytometry analysis (Fig. 1c). Dose-dependent expression of S, S1, and RBD with the expected molecular weight was detected in all infected cells, while none was found in cells infected with the empty vector ChAdTS

(Fig. 1b), as expected. Surface expression of S and intracellular expression of the RBD was further confirmed by staining with the RBD-specific mAbs 1F11 and 2F6, initially isolated from SARS-CoV-2 infected individuals (Fig. 1c). As both of these mAbs recognize conformational epitopes on the RBD, the positive signals indicated proper expression and presentation of RBD epitopes by the infected cells. Here again, dose-dependent expression was also found by both western blot and flow cytometry analysis, while no signal was detected using the negative control antibody VRC01 (Fig. 1c).

To study the immunogenicity of the recombinant vaccines, we inoculated 18 groups of six-week-old BALB/c mice (n = 5 per group) with ChAdTS-S, ChAdTS-RBD, or ChAdTS-RBDs. Each regimen consisted of three single doses (10^{10}, 10^{9}, or 10^{8} vp) administered either through the intranasal (IN) or intramuscular (IM) route. The negative control animals only received a dose of 10^{10} vp of the ChAdTS empty vector. Serum samples were collected every 2 weeks for 8 weeks, and their binding and neutralizing activities against SARS-CoV-2 pseudovirus were analyzed. As shown in Fig. 1, all three recombinant vaccines were able to induce strong and durable antibody responses after a single immunization. Binding affinity for the RBD and neutralizing activity against pseudovirus became detectable 2 weeks after immunization and continued to rise throughout the 8-week period, particularly for the ChAdTS-S group. The speed and magnitude of the antibody response appeared to be more favorable for those in the IN than in the IM group. Furthermore, dose-dependent responses were found for all vaccine candidates, although the effect was less pronounced in the IN group. By week 8 after immunization, the ChAdTS-S animals had an overall average binding ED50 of 6286.0 in the IN and 8585.4 in the IM group. Among the ChAdTS-RBD and ChAdTS-RBDs animals, the corresponding values were 6515.4 and 3527.2,

as well as 7384.2 and 3948.5, respectively. However, the ChAdTS-S animals displayed higher neutralizing activities than those vaccinated with ChAdTS-RBD and ChAdTS-RBDs. Among the animals that received the highest dose, ChAdTS-S elicited an average neutralizing ID50 of 1508.5 in the IN group and 1253.9 in the IM group, which were approximately 10-fold higher than in the animals vaccinated with ChAdTS-RBD (ID50 187.5 for IN and 172.5 for IM) and ChAdTS-RBDs (ID50 165.2 for IN and 115.0 for IM). No detectable binding and neutralizing activities were found among the negative control animals. These results indicate that ChAdTS-S, ChAdTS-RBD, and ChAdTS-RBDs are all immunogenic, but ChAdTS-S appeared to be superior in inducing a binding and neutralizing antibody response in BALB/c mice.

ChAdTS-S induced potent and durable immune responses against SARS-CoV-2 in BALB/c mice We next conducted a more in-depth analysis of the antibody and T-cell responses in animals immunized with the highest dose of ChAdTS-S (10^{10} vp) (Fig. 2). Consistent with what was detected in the pseudovirus neutralization assay, the neutralizing activity against live SARS-CoV-2 became detectable 2 weeks after immunization and continued to rise throughout the 8-week period, although the IN group (FRNT ID50 2260.1) demonstrated higher levels than the IM group (FRNT ID50 957.3). No neutralizing activity was detected in animals vaccinated with the empty ChAdTS vector (Fig. 2a), as expected. The IN group also showed an increasing saliva IgA antibody response against S trimer, which was temporally correlated with the serum neutralizing activity against live SARS-CoV-2. However, no such response was detected in the IM group (Fig. 2b). In terms of total serum IgG binding to the S trimer, the IN and the IM groups displayed similar dynamics in terms of speed and magnitude. By week 8 after immunization, the binding ED50 in the IN group reached as high as

19869.4, and that of the IM group reached 23058 (Fig. 2c). Interestingly, the binding profile of IgG subtypes for the S trimer were dramatically different between the two groups. In the IN group, IgG1 was dominant, followed by IgG2a and IgG2b throughout the entire study period (Fig. 2d). By contrast, IgG2a was dominant in the IM group, followed by IgG1 and IgG2b (Fig. 2e). As a result, the average IgG2a/IgG1 ratios in the IN group remained well below 1, while they were above 1 in the IM group, and continued to increase to as high as 2.8 by week 8 after immunization (Fig. 2f). These results suggest that ChAdTS-S immunization through the IN route induced a predominately Th2-biased response, whereas the IM route elicited a predominately Th1 response. Such biased (dichotomous) immune responses are further supported by the analysis of T-cell responses in immunized animals. Splenocytes collected 1 week after immunization were subjected to interferon (IFN)-γ ELISPOT and intracellular cytokine staining (ICS) analysis. In the IM group, a large number of spot-forming cells (593 SFU per 10^6 splenocytes) were detected after simulation with an overlapping peptide pool of the S protein, whereas those in the IN group (89 SFU per 10^6 splenocytes) demonstrated no discernable differences from the negative control ChAdTS group (33 SFU per 10^6 splenocytes) (Fig. 2g). The ICS results also showed the same trend in the number of $CD8^+$ and $CD4^+$ T cells producing IFN-γ, tumor necrosis factor (TNF)-α, and interleukin (IL)-2 (Fig. 2h and i). These results indicate that a single immunization with ChAdTS-S induces strong antibody and cellular immune responses. The IN route appeared to elicit a predominately Th2 immune response, whereas the IM route elicited an immune response that was more biased toward Th1 cells.

To further study how long the elicited antibody response can persist after a single immunization, we intranasally or intramuscularly inoculated 2 groups of six-week-old

BALB/c mice (n = 10 per group). Within each group, five animals received 10^{10} vp of ChAdTS-S and the remaining five were administered 10^{10} vp of the empty ChAdTS vector as a negative control. Blood samples were collected every two weeks from the time of immunization until 36 weeks thereafter. As shown in Fig. 2j, the titer of binding antibodies against the S trimer increased dramatically two weeks after immunization, continued to increase and remained at high levels in the ensuing period of time. IN and IM immunization appeared to induce equivalently high levels of binding antibodies without an appreciable decline throughout the experiment. Furthermore, the neutralizing antibody response, measured using the pseudovirus neutralization assay, also demonstrated a similar trend of increase and persistence after a single immunization. IN immunization appeared to induce relatively higher levels of neutralizing antibodies than the IM route, although the differences were not statistically significant. These results indicate that a single immunization with ChAdTS-S through either the IN or IM route is able to induce strong and durable antibody response, a unique and advantageous feature compared to other reported strategies.

ChAdTS-S elicited potent and protective immune responses against SARS-CoV-2 in rhesus macaques A total of eight adult rhesus macaques (6 to 9 years old) were immunized with a single inoculum comprising 10^{11} vp of ChAdTS-S either via the IN (n = 4) or the IM route (n=4). Within each group, two animals received ChAdTS-S and the remaining two received the empty ChAdTS vector without any insert (Fig. 3a). From two weeks post vaccination, IgG responses against trimeric S and RBD were detected in all serum samples from the ChAdTS-S-vaccinated animals. In the IN group, the IgG response appeared to be faster and higher than that in the IM group, where a relatively slower but steadily increasing response was observed until challenge (Fig.

3b, c). Trimeric S-specific IgA antibodies were only detectable in serum samples from animals immunized through the IN route (Fig. 3d). However, the IgA response seemed to be short-lived and exhibited a clear decline at two to four weeks after vaccination. Consistent with the binding activity, serum neutralizing antibodies against the pseudovirus and live SARS-CoV-2 became detectable two weeks post vaccination. The IN group also demonstrated faster and higher levels than the IM group, but experienced a dramatic decline in the ensuing period while the antibody titer in the IM group continued to increase or remained relatively stable up to 8 weeks post vaccination (Figs. 3e and f). In addition, all vaccinated and control animals developed low levels of ChAdTS vector-specific neutralizing antibodies, although the IN vaccinated macaques developed relatively lower levels of anti-vector neutralizing antibodies than the IM vaccinated macaques (Fig. 3g), similar to what was reported in Ad5 immunized animals[36]. Finally, serum cytokine profiling at two weeks post vaccination revealed that the IM-vaccinated animals had detectable levels of IFNγ and IL-2, while the IN animals demonstrated high levels of IL-6 and IL-18 (Fig. 3h). At four weeks post vaccination, almost all these cytokines exhibited a precipitous decline, but IL-6 showed an increase instead (Fig. 3i).

To evaluate the protective potential of ChAdTS-S, immunized rhesus macaques were challenged with 10^6 plaque-forming units (PFU) of live SARS-CoV-2 by intratracheal inoculation (Fig. 3a). As the animals in the IN and IM groups responded differently to vaccination, they were challenged either at 4 weeks post vaccination (IN group) or 8 weeks post vaccination (IM group) (Fig. 3a). All animals were euthanized on day 7 (IM group) or 8 (IN group) after the challenge. Viral loads in lung tissues and nasal swabs were quantified, and histopathological analysis of lung tissues was conducted. The absolute number of viral genomic RNA (gRNA) and sub-genomic RNA (sgRNA, an

301 indication of replicating virus) were measured by droplet PCR, which is more sensitive
302 and accurate than conventional RT-PCR[37]. As shown in Fig. 4a, no detectable levels
303 of gRNA or sgRNA were found in the lung tissues of ChAdTS-S-vaccinated macaques,
304 while in the control group the viral load reached as high as 2.37×10^8 and 1.17×10^5
305 copies per gram, respectively. ChAdTS-S-vaccinated animals also demonstrated
306 transient levels of gRNA or sgRNA in the nasal swabs, while the control animals
307 showed persistent high levels throughout the experiments. For example, one animal
308 in the IN group demonstrated gradually decreasing gRNA and sgRNA levels from day
309 2 up to day 7 after the challenge, although the gRNA levels were substantially higher
310 than the sgRNA levels. Similarly, one animal in the IM group also had detectable levels
311 of gRNA and sgRNA on day 2 after challenge, but the viral load became undetectable
312 afterwards. This result may indicate that only a small fraction of detected gRNA copies
313 in the nasal swab are relevant to viral replication. Finally, we performed
314 histopathological analysis on the lung sections collected on day 7 or 8 after the viral
315 challenge. As shown in Fig. 4d, the ChAdTS-S-vaccinated macaques in both the IN
316 and IM groups maintained a normal lung structure with mild infiltration of interstitial
317 lymphocytes and macrophages recruited to the alveolar space. By contrast, the control
318 animals showed severe interstitial pneumonia in all lobes, as evidenced by the
319 infiltration of monocytes and lymphocytes in most alveoli, as well as edema in a
320 proportion of alveoli (Fig. 4d). These results indicate that ChAdTS-S was able to elicit
321 potent and protective immune responses against SARS-CoV-2 infection in rhesus
322 macaques.
323
324 **ChAdTS-S protected golden Syrian hamsters from SARS-CoV-2 infection** We
325 went further to evaluate the protective potential of ChAdTS-S in another animal model

of SARS-CoV-2 infection using golden Syrian hamsters. A total of eight hamsters were intramuscularly inoculated with either 10^{10} vp of ChAdTS-S (n=4) or saline as control (n=4) and monitored for their serum antibody response 2 and 4 weeks after immunization. At 6 weeks post immunization, the animals were challenged with 10^5 PFU of SARS-CoV-2 (HKU-13 strain, GenBank accession no: MT835140) and assessed for body weight changes, viral RNA titer and immunohistochemical staining for viral antigens in the lungs up to 4 days after the challenge. As shown in Fig. 5a and 5b, ChAdTS-S elicited a strong antibody response at 2 and 4 weeks after immunization. Immunization protected the animals from body weight loss (Fig. 5c) and significantly reduced the viral RNA load in the lungs compared to the control animals (Fig. 5d). Immunohistochemistry analysis failed to detect viral nucleocapsid protein in lung sections of ChAdTS-S immunized animals, while immunopositivity was abundantly visible and widely distributed along the alveolar epithelia cells in the control group (Fig. 5e, f). Collectively, these results show that ChAdTS-S is able to elicit protective immunity in the golden Syrian hamster model of SARS-CoV-2 infection.

Neutralization of SARS-CoV-2 variants by immune sera elicited by ChAdTS-S To determine whether immune sera from ChAdTS-S-vaccinated animals could neutralize the SARS-CoV-2 variants of concern, we tested their neutralizing activities against 4 pseudoviruses carrying either the wild type Wuhan-Hu-1 strain, UK501Y.V1 variant (GISAID: EPI_ISL_601443), SA501Y.V2 variant (GISAID: EPI_ISL_792681), and BR501Y.V3 variant (GISAID: EPI_ISL_700450). Both SA501Y.V2 and BR501Y.V3 contain three RBD mutations of concern at positions K417, E484 and N501. The immune sera from BALB/c remains largely unaffected in neutralizing the variants, although the average ID50 against BR501Y.V3 (ID50 1076.9 for IM and 2712.4 for IN)

was relatively higher than that to wildtype Wuhan-Hu-1 (ID50 626.9 for IM and 2207.5 for IN) (Fig. 6a). However, the immune sera from the rhesus macaque serums demonstrated 1 to 3.0-fold decline against SA501Y.V2 and BR501Y.V3, although about 1 to 3.7-fold increase was found against UK501Y.V1 (Fig. 6b). Such discrepancy between mice and rhesus macaque may due to different immune responses induced by the same immunogen ChAdTS-S or limited number of animals studied here. Regardless, immunogenicity and protectivity of the vaccines against newly emerged SARS-CoV-2 variants warrant further investigation.

Discussion

SARS-CoV-2 continues to rage around the world with no sign of abating. One contributing factor is the high prevalence of asymptomatic COVID-19 patients, particularly among the young and healthy population[38,39]. While many public health measures have proven successful in containing viral spread, the ultimate control will rely on the successful development and deployment of safe and effective vaccines against SARS-CoV-2. In this study, we constructed recombinant viral vectors expressing either the S-protein or its RBD based on the rare serotype chimpanzee adenovirus ChAdTS as potential vaccine candidates against SARS-CoV-2 infection. We show that a single IN or IM immunization elicited a robust and sustained neutralizing antibody response in BALB/c mice, with ChAdTS-S being superior to ChAdTS-RBD and ChAdTS-RBDs. IN immunization induced a predominately Th2-biased response, whereas the IM route resulted in a predominately Th1 response in mice. Such biased immune responses are further supported by the analysis of T-cell

responses in the same immunized animals. Interestingly, the neutralizing activity against several circulating SARS-CoV-2 variants remained unaffected for mice serum but reduced for rhesus macaque serum. Such discrepancy between two animal species may reflect different immune responses towards the ChAdTS-S or limited number of animals studied here. Regardless, immunogenicity and protectivity of the vaccines against newly emerged SARS-CoV-2 variants warrant further investigation. Critically, both immunization routes were able to elicit robust and protective immunity in rhesus macaques. Similarly, IM immunization protected golden Syrian hamsters from weight loss, and significantly reduce viral burdens in the lungs and respiratory tract. These results show that ChAdTS-S can induce protective immune responses in experimental animals, confirming that it is a promising candidate for further development of a vaccine against SARS-CoV-2 infection in humans.

A couple of unique aspects of our study can be highlighted here. First and foremost, the ChAdTS vector has desirable properties such as a large capacity for foreign genes and low pre-existing immunity in humans[30,40,41]. This is clearly superior to many adenoviral vectors that are widely used in vaccine development, such as human adenovirus 5 (HuAd5), whose seroprevalence in the normal human population reaches as high as 75-80%[40-44]. This would undoubtedly impose a steep immune barrier for the vector and lead to compromised immunogenicity of the expressed antigen. The only way to overcome such pre-existing immunity is to increase the inoculation dose, but this increases the risk of undesired adverse effects. By contrast, the seroprevalence of ChAdTS is only 0-15%, and even when it is positive, the serum antibody titer is generally low[41,43,44]. This unique feature allows enhanced immunogenicity at low doses of antigens expressed by ChAdTS, thus reducing the likelihood of adverse effects. In fact, the parental AdC68 vector has been engineered

to express antigens from a wide range of pathogens such as Ebola virus, HIV-1 and influenza A virus, demonstrating impressive safety and immunogenicity profiles in preclinical studies[28,29,45-47]. In addition, vaccines based on other serotypes of chimpanzee adenovirus demonstrated similar profiles of low pre-existing immunity. In particular, the ChAdOx1 vaccine expressing the full-length of SARS-CoV-2 S protein (AZD1222), developed by AstraZeneca/Oxford University, has already entered phase III human trials and showed promising safety and efficacy against SARS-CoV-2 infection despite some trial participants only receiving a partial dose[8,9,48,49]. Furthermore, the same adenovirus vector expressing the full-length S protein of MERS-CoV was also evaluated in a phase I human trial and demonstrated good safety and tolerability[4]. ChAd3 vectors expressing Ebola Zaire glycoprotein (ChAd3-EBO-Z) elicited strong immune responses in clinical trial participants[34,35]. These results highlight the favorable safety, tolerability, and immunogenicity profiles of chimpanzee adenovirus vector-based vaccines in humans, which hold great promise for vaccine development.

The second unique aspect of this study is the exceptional durability and strength of the protective immunity elicited by ChAdTS-S in experimental animals. In BALB/c mice, a single IN or IM dose of ChAdTS-S elicited robust and sustained systemic and mucosal immune responses lasting for up to 36 weeks post immunization. Such high and persistent levels of antibodies are superior to many vaccines for which immunogenicity is short-lived and multiple rounds of immunization are required to induce a detectable and protective neutralizing antibody response[1]. While the underlying mechanism is currently unclear, it is possible that the broad host-cell tropism of ChAdTS and the expression of membrane-anchored instead of soluble S protein by the recombinant ChAdTS-S played critical roles. Interestingly, IN

immunization appeared to induce relatively faster and stronger mucosal and systemic antibody responses than IM immunization, although a bias toward the Th2 response was noted. The mucosal response is particularly relevant for protection against SARS-CoV-2 infection, since viral transmission and replication largely occurs in the upper respiratory tract[50]. Intramuscular immunization, however, appeared to induce a more durable antibody response and higher levels of Th1 cells than intranasal immunization. We are currently uncertain whether these differences translate into different levels of protection in mice. However, it is reassuring to find that a single IN or IM dose of ChAdTS-S elicited protective immune responses against SARS-CoV-2 challenge in rhesus macaques. ChAdTS-S-vaccinated macaques had no detectable levels of SARS-CoV-2 gRNA or sgRNA in the lung tissues, with only transient and low levels in the nasal swabs. By contrast, the control animals showed persistent high levels of viral RNA throughout the experiment. ChAdTS-S-vaccinated animals also maintained normal lung structure, while the control animals showed severe interstitial pneumonia in all lobes. Finally, single-dose intramuscular immunization of golden Syrian hamsters with ChAdTS-S also induced robust and protective immunity, which prevented body weight loss and inhibited viral replication in lung tissues according to viral RNA loads and immunohistochemical staining for the SARS-CoV-2 NP protein. Taken together, these results highlight that ChAdTS-S can elicit potent and protective immune responses against SARS-CoV-2 in experimental animals, meriting further translational research toward a clinical vaccine against SARS-CoV-2 infection in humans.

Materials and Methods

Construction, rescue, amplification and purification of ChAdTS-based vaccines

The ChAdTS, derived from AdC68, is an E1- and E3-deleted replication-deficient adenoviral vector. It also has a partial deletion in E4, which was replaced by the corresponding E4 region of the human adenovirus 5 AdHu5[51]. The codon-optimized gene encoding the spike (S) protein from SARS-CoV-2 (Wuhan-Hu-1, GenBank: MN908947.3) was synthesized by Tsingke Biological Technology, China. The coding sequence of the RBD region, which spans the residues Arg319–Phe541 of the S protein, was obtained by PCR from the codon-optimized spike gene. The full-length S protein, RBD with the original signal peptide from the S protein, and RBD with the secretory signal peptide from the mouse Ig heavy chain were inserted into the E1-deleted region of the ChAdTS vector by isothermal assembly to obtain the vectors pChAdTS-S, pChAdTS-RBD, and pChAdTS-RBDs, respectively. The primer pair for ChAdTS-S included the forward primer (5'-gctagcgtttaaacgggcccGCCCGGGCTTATAAgccaccATGTTCCTGCTGACCACC-3') and the reverse primer (5'-agcggtttaaacttaagcttGCCCGGGCTTATAACTAGGTGTAGTGCAGCTTCA-3'). The primer pair for ChAdTS-RBD included the forward primer (5'-gctagcgtttaaacgggcccGCCCGGGCTTATAAgccaccATGTTCGTGTTCCTGGTGCT-3') and the reverse primer (5'-agcggtttaaacttaagcttGCCCGGGCTTATAACTAGAAATTCACGCACTTAT-3'). The primer pair for ChAdTS-RBDs included the forward primer (5'-gctagcgtttaaacgggcccGCCCGGGCTTATAAgccaccATGGGATGGTCATGTATC-3') and the reverse primer (5'-agcggtttaaacttaagcttGCCCGGGCTTATAACTAGAAATTCACGCACTTAT-3'). Empty ChAdTS with no insertion in the E1 deletion region was employed as the negative

control vaccine. The vectors pChAdTS-S, pChAdTS-RBD, and pChAdTS-RBDs were linearized and transfected into HEK293 cells (ATCC) to rescue ChAdTS-S, ChAdTS-RBD, and ChAdTS-RBDs. Theses recombinant adenoviruses as well as empty control ChAdTS were propagated and purified by CsCl gradient ultracentrifugation before quantification by spectrophotometry[51,52].

Detection of S and RBD protein expression HEK293T cells cultured in 6-well plates were infected with ChAdTS-S, ChAdTS-RBD, ChAdTS-RBDs, and ChAdTS at doses of 10^{10}, 10^{9}, and 10^{8} vp per well. After 24 h, the cells were harvested and lysed with 100 μL of buffer containing a protease inhibitor cocktail. The cell lysates were subjected to SDS-PAGE, followed by western blotting with a primary anti-SARS-CoV-2 S antibody (Sino Biological, China) and detected using an HRP-conjugated secondary anti-rabbit IgG (Promega, USA). Beta-actin was used as a loading control. In the flow cytometry assay, S and RBD expression was detected by surface and intracellular staining, respectively. Two human monoclonal antibodies (P2C-1F11 and P2B-2F6)[14] specific for the RBD isolated from SARS-CoV-2 infected individuals were incubated with infected cells at a final concentration of 10 μg/mL at 4°C for 30 min. After extensive washing, the cells were further incubated with anti-human IgG-PE (BioLegend, USA) at a 1:50 dilution and analyzed using a BD Calibur FACS instrument (BD, USA). The VRC01 antibody specific for human immunodeficiency virus type I (HIV-1), was used as a negative control.

Mouse immunization and sample collection A total of 120 female BALB/c mice aged 6–8 weeks were randomly divided into 24 groups (n = 5 in each group) and immunized with a single dose comprising 10^{10}, 10^{9}, or 10^{8} vp of ChAdTS-S, ChAdTS-

RBD, ChAdTS-RBDs, or ChAdTS via either the intranasal (IN) or intramuscular (IM) route. Sera were collected every 2 weeks until 8 weeks following the immunization, heat-inactivated at 56°C for 30min, and stored at -80°C before analysis for SARS-CoV-2 specific antibodies. T cell responses were measured in the spleens of 20 additional female BALB/c mice one week after immunization. To further study the durability of the elicited antibody response, 20 additional female BALB/c mice aged 6–8 weeks were intranasally or intramuscularly immunized with 10^{10} vp of ChAdTS-S and followed up to 36 weeks. Blood samples were collected every 2 weeks, heat-inactivated at 56°C for 30min, and stored at -80°C before analysis for SARS-CoV-2-specific binding and neutralizing antibodies.

Rhesus macaque immunization and challenge with live SARS-CoV-2 Eight adult rhesus macaques aged between 5 and 9 years were intranasally or intramuscularly vaccinated with 10^{11} vp of ChAdTS-S or empty ChAdTS. Peripheral blood samples were collected every 2 weeks for antibody and cytokine profiling. The vaccinated animals were intratracheally challenged with 10^6 PFU of live SARS-CoV-2 after 4 weeks after intranasal or 8 weeks after intramuscular immunization. Nasal swabs were collected on days 0, 1, 2, 3, 5, and 7 after the viral challenge. The animals were euthanized on either day 7 or 8 after the challenge and the lungs were collected for viral load analysis and histopathological examination. Viral gRNA and sgRNA in the lung tissues and nasal swabs were measured by droplet digital PCR[37], using a COVID-19 digital PCR detection kit (TargetingOne, China). The kit allows the detection of the *ORF1ab* gene, *N* gene, and a positive reference gene. The limit of detection is 3 copies/test for *ORF1ab* gene and 5 copies/test for *N* gene. The same detection kit, with different primers and probes to target the *E* gene was used for the detection of

sgRNA[53]. For histopathological analysis, lung tissues were collected and fixed in 10% neutral buffered formalin, embedded in paraffin, and sectioned (5 μm) for standard hematoxylin and eosin staining.

Golden Syrian hamster immunization and challenge with live SARS-CoV-2 The entire procedure was performed as described previously[54]. Briefly, 6- to 8-week-old-male and female hamsters were obtained from the Chinese University of Hong Kong Laboratory Animal Service Centre through the HKU Laboratory Animal Unit and kept in Biosafety Level-2 (BSL-2) housing until virus challenge in the BSL-3 animal facility. The hamsters (n=4 per group) were immunized with ChAdTS-S or saline as control via the IM route. Six weeks later, each hamster was intranasally challenged with a single dose comprising 10^5 PFU of live SARS-CoV-2 (HKU-13 strain, GenBank accession no: MT835140) under intraperitoneal ketamine (200 mg/kg) and xylazine (10 mg/kg) anesthesia. The weights of the hamsters were monitored daily and the animals were sacrificed at day 4 post-challenge. Half of each hamster's lung was used for viral load determination using a quantitative SARS-CoV-2 RdRp/β-actin reverse transcription-polymerase chain reaction assay. For immunostaining, lung tissues were fixed and incubated with a monoclonal antibody against SARS-CoV-2 nucleocapsid (Sino Biological, China).

ELISA of binding antibodies in the sera of immunized mice, rhesus macaques and golden Syrian hamsters For the immunized mice, the serum samples were serially diluted and added to 96-well plates pre-coated with recombinant SARS-CoV-2 S trimer or RBD produced in HEK 293F cells (100 ng/well). After incubation at 37°C for 1 h, the plates were washed three times with phosphate-buffered saline containing

0.1% Tween® 20 (PBST) and incubated with a secondary horseradish peroxidase (HRP)-conjugated antibody against mouse IgG (1:4000, Promega, USA), IgG1, IgG2a, IgG2b, or IgA (1:40000; Abcam, UK) at 37°C for 1 h. The samples were further washed 3 times with PBST before the substrate TMB (3',3',5',5',-tetramethyl benzidine) was added and the reaction was stopped by adding 1M H_2SO_4. Absorbance at 450nm was measured using an ELISA plate reader. The ED50 value was calculated based on binding curves drawn in Prism 8.0 software (GraphPad Inc., USA). For immunized rhesus macaques, the IgG response specific to the SARS-CoV-2 S trimer or RBD was measured using an HRP-conjugated anti-monkey IgG (1:6000; Southern Biotech, USA), but otherwise same as the protocol for the immunized mice (see above). The endpoint antibody titer of the macaque sera was defined as the optical value three times above that of the naïve serum. For immunized golden Syrian hamsters, the antibody response was measured using an HRP-conjugated anti-hamster IgG (Invitrogen, USA).

Pseudovirus and live virus neutralization assays Neutralizing titers of the immunized sera were determined using SARS-CoV-2 pseudovirus and live virus neutralization assays as previously reported[14]. The pseudovirus was generated by co-transfection of HEK293T cells with the HIV backbone expressing firefly luciferase (pNL43R-E-luciferase) and pcDNA3.1 (Invitrogen, USA) encoding S proteins from SARS-CoV-2 variants. The wild type S protein was from Wuhan-Hu-1, GenBank: MN908947.3. The variant UK501Y.V1 (GISAID: EPI_ISL_601443) was constructed with mutations Δ69-70, Δ144, N501Y, A570D, D614G, P681H, T716I, S982A and D1118H. The variant SA501Y.V2 (GISAID: EPI_ISL_792681) was constructed with mutations L18F, D80A, D215G, Δ242-244, S305T, K417N, E484K, N501Y, D614G,

A701V and R246I. The variant BR501Y.V3 (GISAID: EPI_ISL_700450) was constructed with mutations L18F, T20N, P26S, D138Y, R190S, K417N, E484K, N501Y, D614G, H655Y, T1027I and V1176F. After 48h, the cell supernatant containing the pseudovirus was collected, measured and stored at -80C until further use. Serum samples were serially diluted 3-fold in 96-well cell culture plates before SARS-CoV-2 pseudovirus was added and incubated at 37°C for 1h. Approximately 1.5×10^4 Huh7 cells were then added to the serum-pseudovirus mixture and incubated at 37°C for an additional 60 h. The ID50 values were calculated based on the relative light units (Bright-Glo Luciferase Assay Vector System, Promega, USA) using Prism 8.0 (GraphPad Software Inc., USA). For the live virus assay, we used live SARS-CoV-2 initially isolated from an infected patient in China and the focus reduction neutralization was performed in a certified BSL3 facility at Shenzhen Third People's Hospital, China. Briefly, serial dilutions of sera were mixed with SARS-CoV-2 and incubated for 1 h at 37°C. The mixtures were then transferred to 96-well plates seeded with Vero E6 cells and incubated for 1h at 37°C. After changing the medium, the plates were incubated at 37°C for an additional 24h. The cells were then fixed, permeabilized, and incubated with cross-reactive rabbit anti-SARS-CoV-N IgG (Sino Biological, Inc., China) for 1h at room temperature before adding an HRP-conjugated goat anti-rabbit IgG antibody (Jackson ImmunoResearch, USA). The reactions were developed using KPL TrueBlue peroxidase substrate (Seracare Life Sciences Inc., USA). The number of SARS-CoV-2 foci was quantified using an EliSpot reader (Cellular Technology Ltd. USA).

Adenovirus neutralization assay The levels of chimpanzee adenovirus-specific neutralizing antibodies were measured as described previously[42]. Serum samples

were 3-fold serially diluted in 96-well cell culture plates and mixed with 1500 $TCID_{50}$ of ChAdTS-GFP vector, which expresses green fluorescent protein. After incubation at 37 °C for 1 h, approximately 1.5×10^4 HEK293 cells were added to the antibody-virus mixture and co-cultured for an additional 24 h. The green fluorescent protein levels were examined using an Opera Phenix (PerkinElmer, USA) to determine the levels of vector-specific neutralizing antibodies. The ID_{50} values of the sera for ChAdTS were defined as the dilution required to reduce the number of GFP-expressing cells by 50% compared with wells treated with the virus alone.

Assessment of T-cell responses in mice Cellular immune responses in the vaccinated mice were assessed using the IFN-γ pre-coated ELISPOT kit (MabTech, Sweden), according to the manufacturer's protocol. Splenocytes from mice were stimulated with a peptide pool covering the SARS-CoV-2 S protein (GenScript, USA) at a concentration of 2 μg/mL of each peptide. Phorbol myristate acetate/ionomycin was used as a positive control and RPMI 1640 medium as a negative control. After incubation at 37°C for 28 h, the plates were washed extensively before a biotinylated anti-mouse IFN-γ antibody was added to each well and incubated further for 2 h at room temperature. The substrate AEC was added and the spots in each well were read using the automated ELISPOT reader (AID, USA). The number of spot-foring units (SFUs) per 1,000,000 cells was calculated. For T cell proliferation analysis, approximately 1,000,000 mouse splenocytes were stimulated with the same SARS-CoV-2 S peptide pool as above (2 μg/mL of each peptide) and brefeldin A (GolgiPlug; BD, USA) for 6 h at 37 °C in 5% CO_2. Following two washes with PBS, the splenocytes were permeabilized and stained with the fluorescently conjugated antibodies CD4-FITC (GK1.5; BioLegend, USA), CD8-PE/Cyanine7 (53-6.7; BD), CD19-

APC/Cyanine7 (1D3; BD), INFγ-BV421 (XMG1.2; BD), TNFα-APC (MP6-XT22; BioLegend), and IL2-PE (JES6-5H4, BioLegend). Dead cells were stained using the Zombie Yellow Fixable Viability Kit (BioLegend, USA). The data were collected using a Cytek Aurora FACS instrument (Cytek, USA) and analyzed using FlowJo software.

Ethics statement All experiments were carried out in strict compliance with the Guide for the Care and Use of Laboratory Animals of the People's Republic of China and approved by the Committee on the Ethics of Animal Experiments of Tsinghua University, Chinese Academy of Medical Sciences, and University of Hong Kong. Mouse immunization and characterization were conducted in the animal facility of Tsinghua University. Golden Syrian hamster experiments involving live SARS-CoV-2 were conducted in the ABSL-3 facility at the University of Hong Kong. Rhesus macaque experiments involving live SARS-CoV-2 were performed in the ABSL-4 facility of the Kunming National High-level Biosafety Primate Research Center, Yunnan, China, and approved by the institutional biosafety committee.

Statistical analysis Prism 8.0 software (GraphPad, USA) was used for statistical analysis and data plotting. Unless specified otherwise, the data are presented as means ± SEM. Analysis of unpaired Students' *t*-test (two-tailed) was used to determine the statistical significance of differences among different groups (*P < 0.05; **P < 0.01; ***P < 0.001; ****P < 0.0001; n.s., not significant).

Acknowledgements

This work was chiefly supported by funds from the National Key Plan for Scientific Research and Development of China (2020YFC0848800, 2020YFC0844200,

2018ZX10731101-002, 2017ZX10201101, 2016YFD0500307), the Beijing Advanced Innovation Center for Structural Biology, National Natural Science Foundation of China (31870922, 32070926, 81530065 and 91442127), and the Science and Technology Innovation Committee of Shenzhen Municipality (202002073000002). It was also supported by Tsinghua University Initiative Scientific Research Program (20201080053), Beijing Municipal Science and Technology Commission (171100000517-001 and -003), and Tsinghua University Spring Breeze Fund (2020Z99CFG004), as well as Tencent Foundation, Shuidi Foundation, and TH Capital. ZC and HC are partially supported by the InnoHK CVVT program.

Author Contributions

D.Z. and L.Z. conceived, designed, and supervised the entire study. M.L., G.J., H.S., M.X. and W.J. constructed, produced and purified the vaccines and carried out all immunogenicity evaluations in mice. S.L., H. L., and X. P. performed the immunization and protection experiment in rhesus macaques. R. Z., P.W., L.L., S.L., H.C. and Z. C. performed the immunization and protection experiments in golden Syrian hamsters. Q.L., L.F., Q.Z. and X.S. assisted the mouse immunization and evaluation experiments. L.C., B.J., and Z.Z. carried out the live virus neutralization assays. N.W. and Y.G. carried out the droplet digital PCR. Y.W. and H. Q. assisted the intracellular cytokine staining assays. R.W. made the construction of S variants. Z.H., X.T. and L.Y. are employees of Walvax Biotechnology Co., Ltd. M.L., G.J., D.Z. and L.Z. wrote the manuscript. All other authors reviewed and edited the manuscript.

Competing Interests

The authors declare that L.Z., D.Z., M.L. and X.S. are co-inventors on pending patent applications related to the ChAdTS-S, ChAdTS-RBD, and ChAdTS-RBDs vaccine candidates. Z.H., X.T. and L.Y. are employees of Walvax Biotechnology Co., Ltd. The remaining authors declare no competing interests.

References

1. Dagotto, G., Yu, J. & Barouch, D.H. Approaches and Challenges in SARS-CoV-2 Vaccine Development. *Cell Host Microbe* **28**, 364-370 (2020).
2. Wang, F., Kream, R.M. & Stefano, G.B. An Evidence Based Perspective on mRNA-SARS-CoV-2 Vaccine Development. *Med Sci Monit* **26**, e924700 (2020).
3. Maruggi, G., Zhang, C.L., Li, J.W., Ulmer, J.B. & Yu, D. mRNA as a Transformative Technology for Vaccine Development to Control Infectious Diseases. *Mol Ther* **27**, 757-772 (2019).
4. Folegatti, P.M.*, et al.* Safety and immunogenicity of a candidate Middle East respiratory syndrome coronavirus viral-vectored vaccine: a dose-escalation, open-label, non-randomised, uncontrolled, phase 1 trial. *Lancet Infect Dis* **20**, 816-826 (2020).
5. Barouch, D.H.*, et al.* Evaluation of a mosaic HIV-1 vaccine in a multicentre, randomised, double-blind, placebo-controlled, phase 1/2a clinical trial (APPROACH) and in rhesus monkeys (NHP 13-19). *Lancet* **392**, 232-243 (2018).
6. Dong, Y.*, et al.* A systematic review of SARS-CoV-2 vaccine candidates. *Signal Transduct Target Ther* **5**, 237 (2020).
7. Poland, G.A., Ovsyannikova, I.G. & Kennedy, R.B. SARS-CoV-2 immunity: review and applications to phase 3 vaccine candidates. *Lancet* **396**, 1595-1606 (2020).
8. Tebas, P.*, et al.* Safety and immunogenicity of INO-4800 DNA vaccine against SARS-CoV-2: A preliminary report of an open-label, Phase 1 clinical trial. *EClinicalMedicine*, 100689 (2020).
9. Voysey, M.*, et al.* Safety and efficacy of the ChAdOx1 nCoV-19 vaccine (AZD1222) against SARS-CoV-2: an interim analysis of four randomised controlled trials in Brazil, South Africa, and the UK. *Lancet* **397**, 99-111 (2021).
10. Zhu, F.C.*, et al.* Immunogenicity and safety of a recombinant adenovirus type-5-vectored COVID-19 vaccine in healthy adults aged 18 years or older: a randomised, double-blind, placebo-controlled, phase 2 trial. *Lancet* **396**, 479-488 (2020).
11. Walls, A.C.*, et al.* Structure, Function, and Antigenicity of the SARS-CoV-2 Spike Glycoprotein. *Cell* **181**, 281-292 e286 (2020).
12. Hoffmann, M.*, et al.* SARS-CoV-2 Cell Entry Depends on ACE2 and TMPRSS2 and Is Blocked by a Clinically Proven Protease Inhibitor. *Cell* **181**, 271-+ (2020).

13. Lan, J., *et al.* Structure of the SARS-CoV-2 spike receptor-binding domain bound to the ACE2 receptor. *Nature* **581**, 215-+ (2020).
14. Ju, B., *et al.* Human neutralizing antibodies elicited by SARS-CoV-2 infection. *Nature* **584**, 115-+ (2020).
15. Liu, L., *et al.* Potent Neutralizing Monoclonal Antibodies Directed to Multiple Epitopes on the SARS-CoV-2 Spike. *bioRxiv* (2020).
16. Yang, J., *et al.* A vaccine targeting the RBD of the S protein of SARS-CoV-2 induces protective immunity. *Nature* **586**, 572-577 (2020).
17. Wrapp, D., *et al.* Structural Basis for Potent Neutralization of Betacoronaviruses by Single-Domain Camelid Antibodies. *Cell* **181**, 1004-1015 e1015 (2020).
18. Hansen, J., *et al.* Studies in humanized mice and convalescent humans yield a SARS-CoV-2 antibody cocktail. *Science* **369**, 1010-1014 (2020).
19. Wang, Q.H., *et al.* Structural and Functional Basis of SARS-CoV-2 Entry by Using Human ACE2. *Cell* **181**, 894-+ (2020).
20. Shang, J., *et al.* Structural basis of receptor recognition by SARS-CoV-2. *Nature* **581**, 221-+ (2020).
21. Yan, R.H., *et al.* Structural basis for the recognition of SARS-CoV-2 by full-length human ACE2. *Science* **367**, 1444-+ (2020).
22. Shi, R., *et al.* A human neutralizing antibody targets the receptor-binding site of SARS-CoV-2. *Nature* **584**, 120-+ (2020).
23. Cao, Y., *et al.* Potent Neutralizing Antibodies against SARS-CoV-2 Identified by High-Throughput Single-Cell Sequencing of Convalescent Patients' B Cells. *Cell* **182**, 73-84 e16 (2020).
24. Rogers, T.F., *et al.* Isolation of potent SARS-CoV-2 neutralizing antibodies and protection from disease in a small animal model. *Science* **369**, 956-963 (2020).
25. Wu, Y., *et al.* A noncompeting pair of human neutralizing antibodies block COVID-19 virus binding to its receptor ACE2. *Science* **368**, 1274-1278 (2020).
26. Ge, J., *et al.* Antibody neutralization of SARS-CoV-2 through ACE2 receptor mimicry. *Nat Commun* **12**, 250 (2021).
27. Jia, W., *et al.* Single intranasal immunization with chimpanzee adenovirus-based vaccine induces sustained and protective immunity against MERS-CoV infection. *Emerg Microbes Infect* **8**, 760-772 (2019).
28. Wang, X., *et al.* Both haemagglutinin-specific antibody and T cell responses induced by a chimpanzee adenoviral vaccine confer protection against influenza H7N9 viral challenge. *Sci Rep* **7**, 1854 (2017).
29. Yang, X., *et al.* Chimpanzee adenoviral vector prime-boost regimen elicits potent immune responses against Ebola virus in mice and rhesus macaques. *Emerg Microbes Infect* **8**, 1086-1097 (2019).
30. Guo, J., Mondal, M. & Zhou, D. Development of novel vaccine vectors: Chimpanzee adenoviral vectors. *Hum Vaccin Immunother* **14**, 1679-1685 (2018).
31. Sheehy, S.H., *et al.* ChAd63-MVA-vectored blood-stage malaria vaccines targeting MSP1 and AMA1: assessment of efficacy against mosquito bite challenge in humans. *Mol Ther* **20**, 2355-2368 (2012).
32. Hartnell, F., *et al.* A Novel Vaccine Strategy Employing Serologically Different Chimpanzee Adenoviral Vectors for the Prevention of HIV-1 and HCV Coinfection. *Front Immunol* **9**, 3175 (2018).
33. Rampling, T., *et al.* Safety and efficacy of novel malaria vaccine regimens of RTS,S/AS01B alone, or with concomitant ChAd63-MVA-vectored vaccines expressing ME-TRAP. *NPJ Vaccines* **3**, 49 (2018).

34. Ewer, K.*, et al.* A Monovalent Chimpanzee Adenovirus Ebola Vaccine Boosted with MVA. *N Engl J Med* **374**, 1635-1646 (2016).
35. Tapia, M.D.*, et al.* Safety, reactogenicity, and immunogenicity of a chimpanzee adenovirus vectored Ebola vaccine in adults in Africa: a randomised, observer-blind, placebo-controlled, phase 2 trial. *Lancet Infect Dis* **20**, 707-718 (2020).
36. Feng, L.*, et al.* An adenovirus-vectored COVID-19 vaccine confers protection from SARS-COV-2 challenge in rhesus macaques. *Nat Commun* **11**, 4207 (2020).
37. Yu, F.*, et al.* Quantitative Detection and Viral Load Analysis of SARS-CoV-2 in Infected Patients. *Clin Infect Dis* **71**, 793-798 (2020).
38. Hu, B., Guo, H., Zhou, P. & Shi, Z.L. Characteristics of SARS-CoV-2 and COVID-19. *Nat Rev Microbiol* (2020).
39. Pollard, C.A., Morran, M.P. & Nestor-Kalinoski, A.L. The COVID-19 pandemic: a global health crisis. *Physiol Genomics* **52**, 549-557 (2020).
40. Chen, H.*, et al.* Adenovirus-based vaccines: comparison of vectors from three species of adenoviridae. *J Virol* **84**, 10522-10532 (2010).
41. Zhang, S.*, et al.* Seroprevalence of neutralizing antibodies to human adenoviruses type-5 and type-26 and chimpanzee adenovirus type-68 in healthy Chinese adults. *J Med Virol* **85**, 1077-1084 (2013).
42. Wang, X.*, et al.* Neutralizing antibody responses to enterovirus and adenovirus in healthy adults in China. *Emerg Microbes Infect* **3**, e30 (2014).
43. Ersching, J.*, et al.* Neutralizing antibodies to human and simian adenoviruses in humans and New-World monkeys. *Virology* **407**, 1-6 (2010).
44. Zhao, H.*, et al.* Seroprevalence of Neutralizing Antibodies against Human Adenovirus Type-5 and Chimpanzee Adenovirus Type-68 in Cancer Patients. *Front Immunol* **9**, 335 (2018).
45. Fitzgerald, J.C.*, et al.* A simian replication-defective adenoviral recombinant vaccine to HIV-1 gag. *J Immunol* **170**, 1416-1422 (2003).
46. Tang, X.*, et al.* Recombinant Adenoviruses Displaying Matrix 2 Ectodomain Epitopes on Their Fiber Proteins as Universal Influenza Vaccines. *J Virol* **91**(2017).
47. Zhang, H.*, et al.* Adenovirus-mediated artificial MicroRNAs targeting matrix or nucleoprotein genes protect mice against lethal influenza virus challenge. *Gene Ther* **22**, 653-662 (2015).
48. Barrett, J.R.*, et al.* Phase 1/2 trial of SARS-CoV-2 vaccine ChAdOx1 nCoV-19 with a booster dose induces multifunctional antibody responses. *Nat Med* (2020).
49. Ramasamy, M.N.*, et al.* Safety and immunogenicity of ChAdOx1 nCoV-19 vaccine administered in a prime-boost regimen in young and old adults (COV002): a single-blind, randomised, controlled, phase 2/3 trial. *Lancet* **396**, 1979-1993 (2021).
50. Zou, L.*, et al.* SARS-CoV-2 Viral Load in Upper Respiratory Specimens of Infected Patients. *N Engl J Med* **382**, 1177-1179 (2020).
51. Yang, Y., Chi, Y., Tang, X., Ertl, H.C.J. & Zhou, D. Rapid, Efficient, and Modular Generation of Adenoviral Vectors via Isothermal Assembly. *Curr Protoc Mol Biol* **113**, 16 26 11-16 26 18 (2016).
52. Wang, X.*, et al.* Adenovirus delivery of encoded monoclonal antibody protects against different types of influenza virus infection. *NPJ Vaccines* **5**, 57 (2020).
53. Wolfel, R.*, et al.* Virological assessment of hospitalized patients with COVID-2019. *Nature* **581**, 465-469 (2020).

54. Chan, J.F., *et al.* Simulation of the Clinical and Pathological Manifestations of Coronavirus Disease 2019 (COVID-19) in a Golden Syrian Hamster Model: Implications for Disease Pathogenesis and Transmissibility. *Clin Infect Dis* **71**, 2428-2446 (2020).

Figure legends

Figure 1. Generation and characterization of recombinant ChAdTS expressing the full-length spike protein or RBD of SARS-CoV-2. (a) Schematic diagram of the recombinant ChAdTS expressing the full-length S protein with its original signal peptide (ChAdTS-S), RBD with the original signal peptide from the S protein (ChAdTS-RBD), or RBD with the secretory signal peptide from mouse IgG (ChAdTS-RBDs). The coding sequence of the S protein or RBD was inserted into the E1 region of the ChAdTS vector under the control of the CMV promoter and terminated using a bovine growth hormone (BGH) polyadenylation signal sequence. **(b)** Western blot analysis of S and RBD expression in HEK293T cells infected with the recombinant ChAdTS (10^8, 10^9 and 10^{10} vp). **(c)** Flow cytometry analysis of S and RBD expression using the SARS-CoV-2-specific mAbs P2C-1F11 and P2B-2F6. HEK293T cell lysates and intact HEK293T cells infected with the empty ChAdTS vector (10^{10} vp) were used as negative controls. VRC01 was used as a negative control antibody. Serum binding activity to SARS-CoV-2 RBD **(d, e, f)** and neutralizing activity against pseudotyped SARS-CoV-2 **(g, h, i)** over an 8-week period after single-dose immunization with ChAdTS-S, ChAdTS-RBD or ChAdTS-RBDs. For each recombinant ChAdTS construct, three different doses (10^{10}, 10^9, and 10^8 vp) were administered through either the intranasal (IN) or intramuscular (IM) route, which is indicated by different

841 symbols and colors. Data points corresponding to animals in the empty ChAdTS vector
842 control groups (10^{10} vp) are shown in grey. All data are presented as means ± SEM.
843
844 **Figure 2. ChAdTS-S induces strong and durable immune responses in BALB/c**
845 **mice.** Animals immunized with 10^{10} vp of ChAdTS-S were characterized in greater
846 detail. **(a)** Neutralizing activity of the immunized serum against live SARS-CoV-2 over
847 an 8-week period after immunization. **(b)** Binding activity of total saliva IgA and **(c)**
848 immune serum total IgG with the SARS-CoV-2 S trimer. Binding activity of immune
849 serum IgG subtypes IgG1, IgG2a, and IgG2b with the SARS-CoV-2 S trimer in the **(d)**
850 IN or **(e)** IM group**. (f)** The IgG2a/IgG1 ratios in the IN and IM groups. **(g)** ELISPOT
851 analysis for IFN-γ-positive splenocytes and FACS analysis of intracellular IFN-γ, TNF-
852 α, and IL-2 production in **(h)** $CD8^+$ and **(i)** $CD4^+$ splenic T cells two weeks after
853 immunization. The durability of the antibody response was analyzed using **(j)** ELISA
854 with the SARS-CoV-2 S trimer and **(k)** pseudovirus neutralization up to 36 weeks after
855 single-dose immunization. Data corresponding to animals in the IN group are shown
856 in red, those in the IM group in blue, and those in the control group in grey. All data
857 are presented as the means ± SEM. Analysis of unpaired Students' *t*-test (two-tailed)
858 was used to determine the statistical significance of differences among different
859 groups (*P < 0.05; **P < 0.01; ***P < 0.001; ****P < 0.0001; n.s., not significant).
860
861 **Figure 3. ChAdTS-S induces strong immune responses in rhesus macaques. (a)**
862 Timeline for vaccination followed by virological and immunological characterization in
863 two groups of animals. In group one, four animals were intranasally immunized with
864 10^{11} vp of ChAdTS-S (n=2) or 10^{11} vp of the empty ChAdTS vector (n=2). After 4
865 weeks post-immunization, the animals were challenged with 10^6 PFU of live SARS-

CoV-2. In group two, the same protocol was followed except that immunization was conducted via the IM route and challenge was carried out 8 weeks after immunization. Blood samples were collected every 2 weeks before viral challenge. Blood samples and nasal swabs were also collected on days 0, 1, 2, 3, 5, and 7 after the challenge. All animals were euthanized on day 7 or 8 after the challenge to quantify the viral load in the lung tissue and conduct histopathological examinations. Binding activity of immune serum total IgG with the SARS-CoV-2 S trimer **(b)**, SARS-CoV-2 RBD **(c)**, or total IgA with the SARS-CoV-2 S trimer **(d)**. Neutralizing activity of immunized serum against pseudovirus **(e)** and live SARS-CoV-2 **(f)**. Neutralizing activity of immunized serum against the empty ChAdTS vector was assessed using a ChAdTS-GFP neutralization assay **(g)**. Serum levels of cytokines were measured on week 2 **(h)** and week 4 **(i)** after immunization. Data corresponding to animals in the IN group are shown in red, those in the IM group in blue, and those in the control group in grey. All data are presented as the means ± SEM.

Figure 4. Vaccination with ChAdTS-S elicits a protective immune response against SARS-CoV-2 infection in rhesus macaques. (a) The total number of viral gRNA and sgRNA copies in lung tissue samples from six lobes was quantified by droplet digital PCR (TargetingOne, China). **(b)** Viral gRNA and **(c)** sgRNA in the nasal swabs were monitored and quantified using the same technique up to day 7 after viral challenge. **(d)** Histopathological comparison of tissues from animals vaccinated with ChAdTS-S and the empty ChAdTS vector animals. Representative tissue sections in standard hematoxylin and eosin staining are shown (10×). The scale bar is 100 μm. Data corresponding to animals in the IN group are shown in red, those in the IM group in blue, and those in the control group in grey. All data are presented as means ± SEM.

Figure 5. Vaccination with ChAdTS-S elicits a protective immune response against SARS-CoV-2 infection in golden Syrian hamsters. The hamsters were immunized with ChAdTS-S (n=4) or saline as control (n=4) via the IM route. **(a)** The binding ability of the immunized serum for SARS-CoV-2 RBD on week 2 and week 4 after immunization was assessed. **(b)** The neutralizing ability of the serum against SARS-CoV-2 pseudovirus. Intranasal challenge with 10^5 plaque-forming units (PFU) of the HKU-13 strain of SARS-CoV-2 was carried out at 6 weeks post immunization. **(c)** Weight loss in SARS-CoV-2 challenged hamsters. Four days after the challenge, lung tissues were harvested to quantify the viral load using qPCR **(d)** and by immunostaining lung tissue sections using a specific monoclonal antibody against SARS-CoV-2 nucleocapsid protein (20×) **(e,f)**. Data corresponding to animals in the IM group in blue, and those in the control group in grey. All data are presented as the means ± SEM. Analysis of unpaired Students' *t*-test (two-tailed) was used (*P < 0.05; **P < 0.01; ***P < 0.001).

Figure 6. Neutralization titers of immune sera from vaccinated BALB/c mice and rhesus macaques against wildtype and new variants of SARS-CoV-2. Sera samples were collected and analyzed against pseudoviruses carrying S protein either from wildtype Wuhan-Hu-1, UK501Y.V1, SA501Y.V2 or BR501Y.V3. **(a)** Neutralizing activity of immune sera from BALB/c mice 36 weeks post immunization and **(b)** from rhesus macaques 2 weeks post IN immunization and 6 weeks post IM immunization. All data are presented as the means ± SEM. Analysis of unpaired Students' *t*-test (two-tailed) was used.

Fig.1

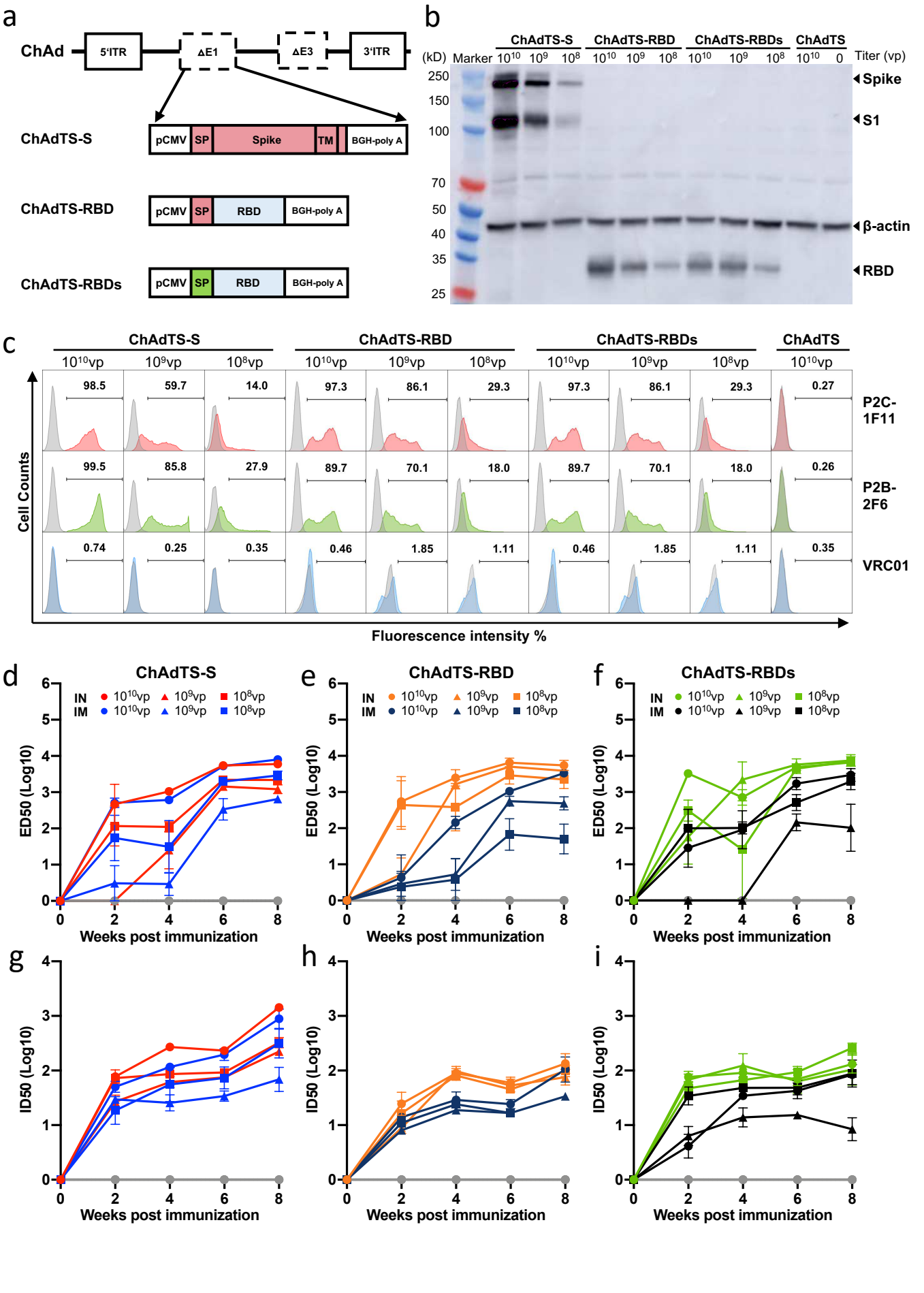
a
ChAd
5'ITR
ΔE1
ΔE3
3'ITR
ChAdTS-S
pCMV
SP
Spike
TM
BGH-poly A
ChAdTS-RBD
RBD
ChAdTS-RBDs
b
ChAdTS-S
ChAdTS-RBD
ChAdTS-RBDs
ChAdTS
(kD)
Marker
Titer (vp)
250
150
100
70
50
40
35
25
Spike
S1
β-actin
RBD
c
ChAdTS-S
ChAdTS-RBD
ChAdTS-RBDs
ChAdTS
10¹⁰vp
10⁹vp
10⁸vp
98.5
59.7
14.0
97.3
86.1
29.3
97.3
86.1
29.3
0.27
P2C-1F11
99.5
85.8
27.9
89.7
70.1
18.0
89.7
70.1
18.0
0.26
P2B-2F6
0.74
0.25
0.35
0.46
1.85
1.11
0.46
1.85
1.11
0.35
VRC01
Cell Counts
Fluorescence intensity %
d
ChAdTS-S
e
ChAdTS-RBD
f
ChAdTS-RBDs
IN
IM
ED50 (Log10)
Weeks post immunization
g
h
i
ID50 (Log10)

Fig.2

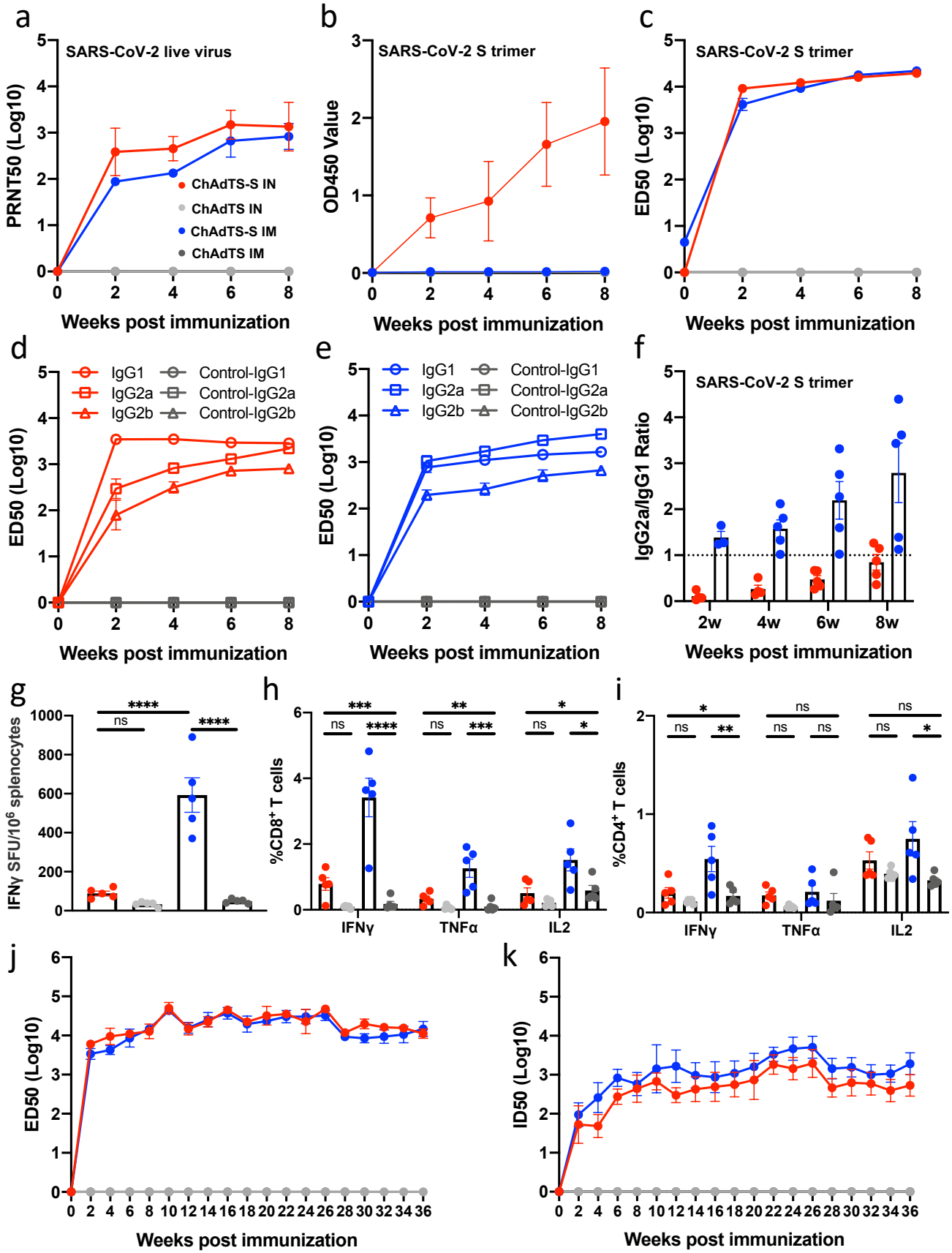
a
SARS-CoV-2 live virus
PRNT50 (Log10)
ChAdTS-S IN
ChAdTS IN
ChAdTS-S IM
ChAdTS IM
Weeks post immunization
b
SARS-CoV-2 S trimer
OD450 Value
Weeks post immunization
c
SARS-CoV-2 S trimer
ED50 (Log10)
Weeks post immunization
d
IgG1
IgG2a
IgG2b
Control-IgG1
Control-IgG2a
Control-IgG2b
ED50 (Log10)
Weeks post immunization
e
IgG1
IgG2a
IgG2b
Control-IgG1
Control-IgG2a
Control-IgG2b
ED50 (Log10)
Weeks post immunization
f
SARS-CoV-2 S trimer
IgG2a/IgG1 Ratio
2w
4w
6w
8w
Weeks post immunization
g
IFNγ SFU/10⁶ splenocytes
****
ns
****
h
%CD8⁺ T cells
***
ns
****
**
ns
***
*
ns
*
IFNγ
TNFα
IL2
i
%CD4⁺ T cells
*
ns
**
ns
ns
ns
ns
*
IFNγ
TNFα
IL2
j
ED50 (Log10)
Weeks post immunization
k
ID50 (Log10)
Weeks post immunization

Fig.3

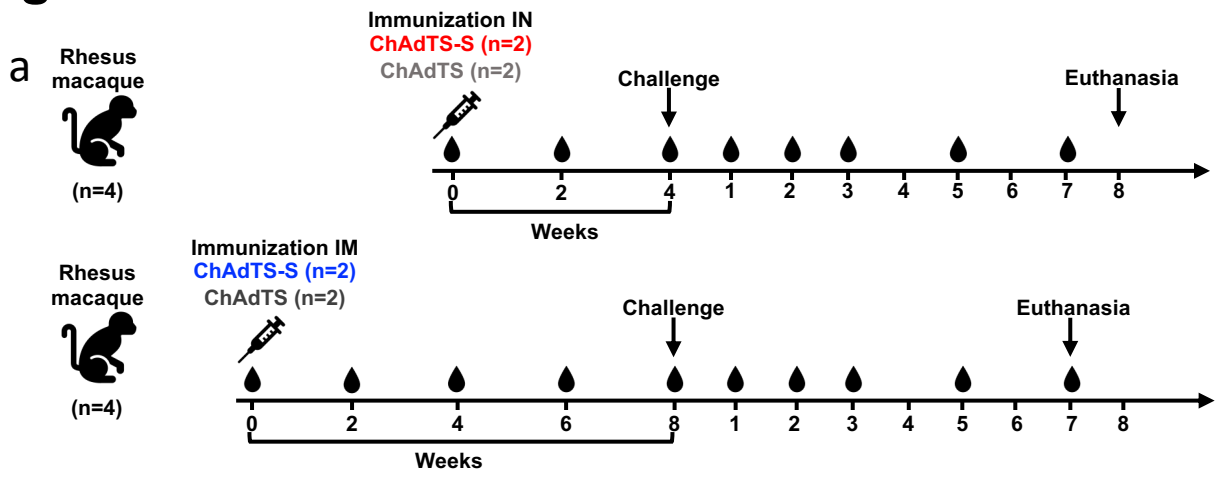
a
Rhesus macaque
(n=4)
Immunization IN
ChAdTS-S (n=2)
ChAdTS (n=2)
Challenge
Euthanasia
0 2 4 1 2 3 4 5 6 7 8
Weeks
Rhesus macaque
(n=4)
Immunization IM
ChAdTS-S (n=2)
ChAdTS (n=2)
Challenge
Euthanasia
0 2 4 6 8 1 2 3 4 5 6 7 8
Weeks

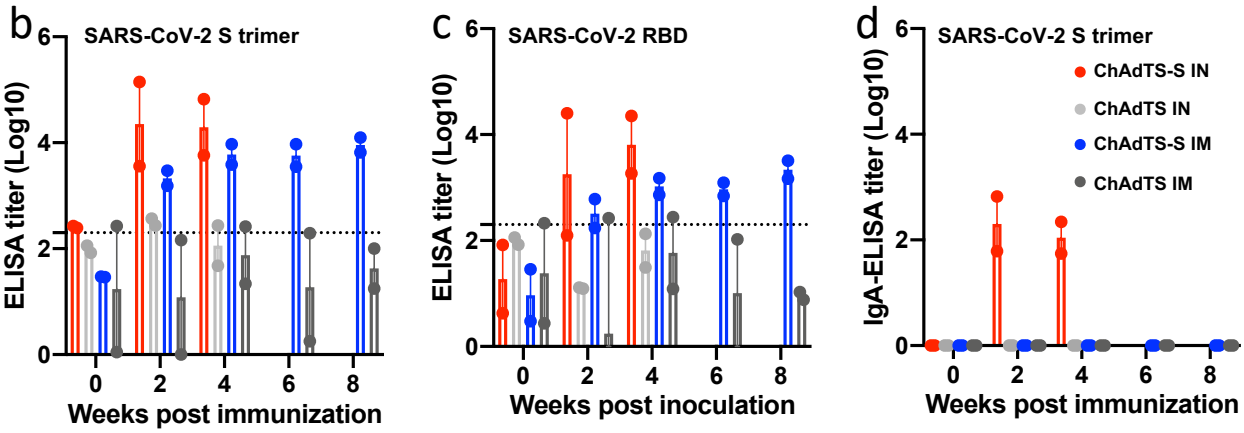
b
SARS-CoV-2 S trimer
ELISA titer (Log10)
Weeks post immunization
c
SARS-CoV-2 RBD
ELISA titer (Log10)
Weeks post inoculation
d
SARS-CoV-2 S trimer
ChAdTS-S IN
ChAdTS IN
ChAdTS-S IM
ChAdTS IM
IgA-ELISA titer (Log10)
Weeks post immunization

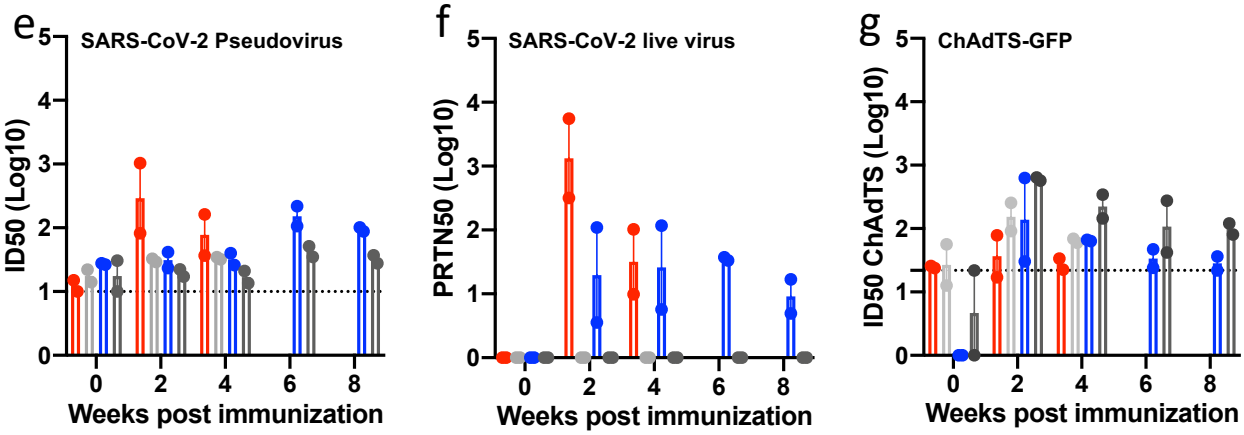
e
SARS-CoV-2 Pseudovirus
ID50 (Log10)
Weeks post immunization
f
SARS-CoV-2 live virus
PRTN50 (Log10)
Weeks post immunization
g
ChAdTS-GFP
ID50 ChAdTS (Log10)
Weeks post immunization

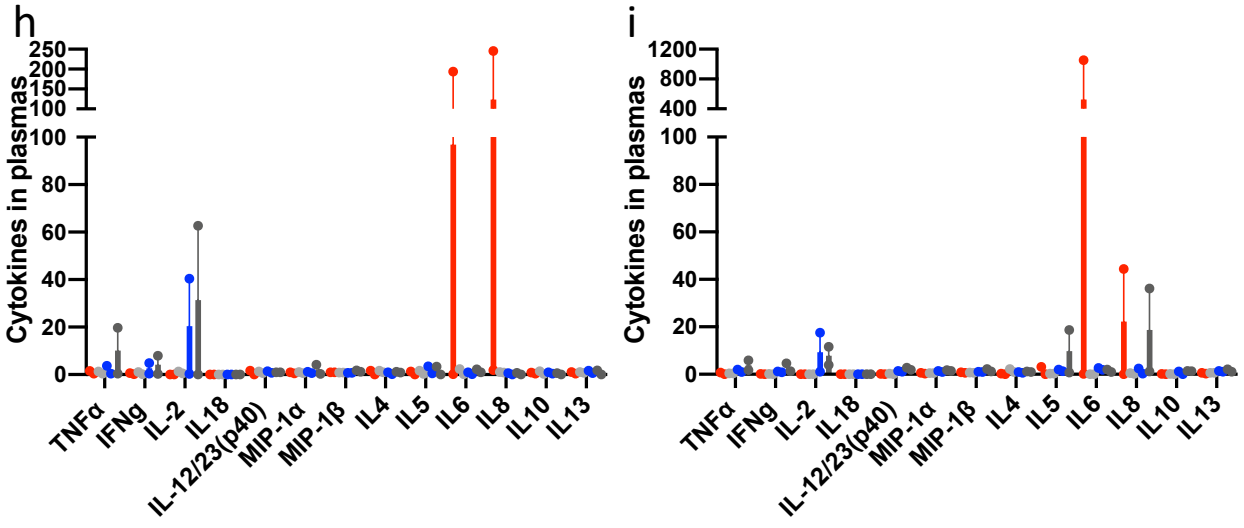
h
Cytokines in plasmas
TNFα
IFNg
IL-2
IL18
IL-12/23(p40)
MIP-1α
MIP-1β
IL4
IL5
IL6
IL8
IL10
IL13
i
Cytokines in plasmas
TNFα
IFNg
IL-2
IL18
IL-12/23(p40)
MIP-1α
MIP-1β
IL4
IL5
IL6
IL8
IL10
IL13

Fig.4

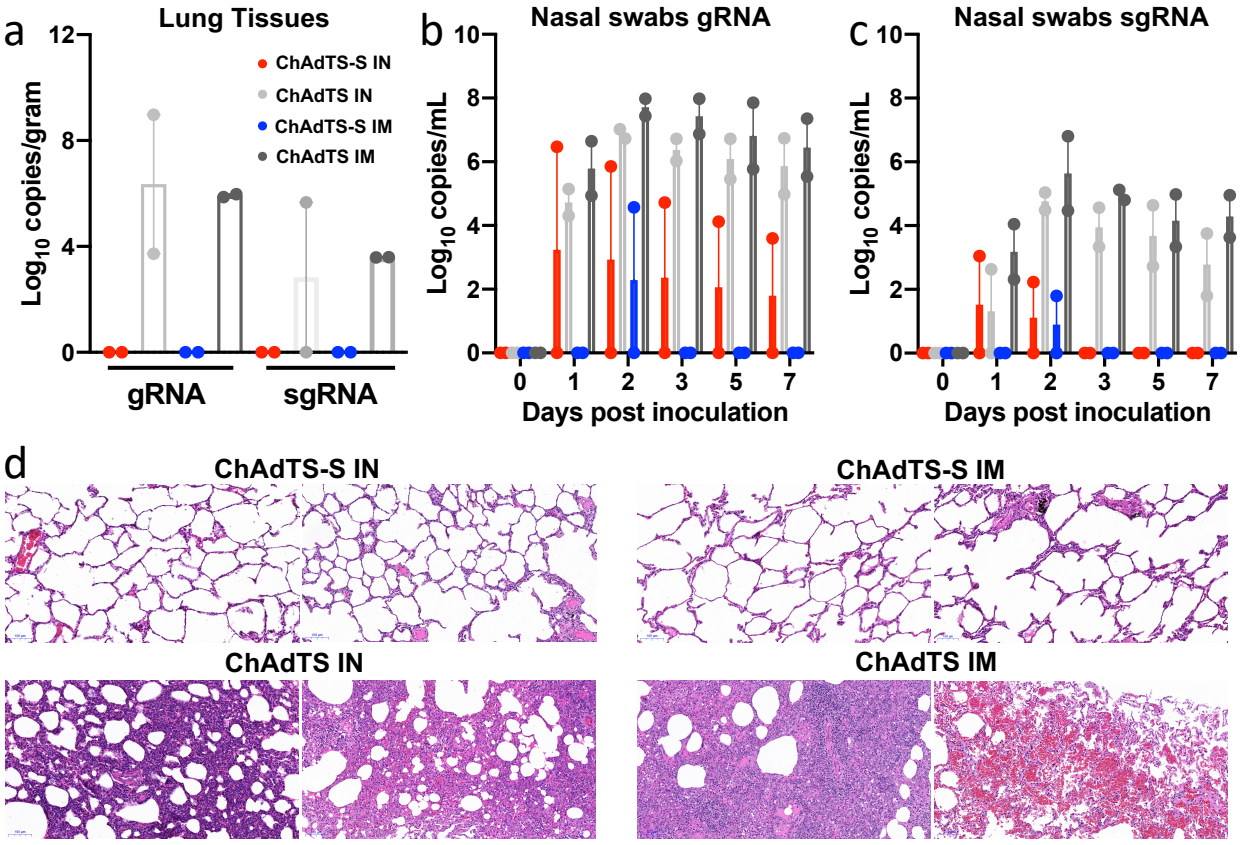
a
Lung Tissues
ChAdTS-S IN
ChAdTS IN
ChAdTS-S IM
ChAdTS IM
Log10 copies/gram
12
8
4
0
gRNA
sgRNA
b
Nasal swabs gRNA
Log10 copies/mL
10
8
6
4
2
0
0
1
2
3
5
7
Days post inoculation
c
Nasal swabs sgRNA
Log10 copies/mL
10
8
6
4
2
0
0
1
2
3
5
7
Days post inoculation
d
ChAdTS-S IN
ChAdTS-S IM
ChAdTS IN
ChAdTS IM

Fig.5

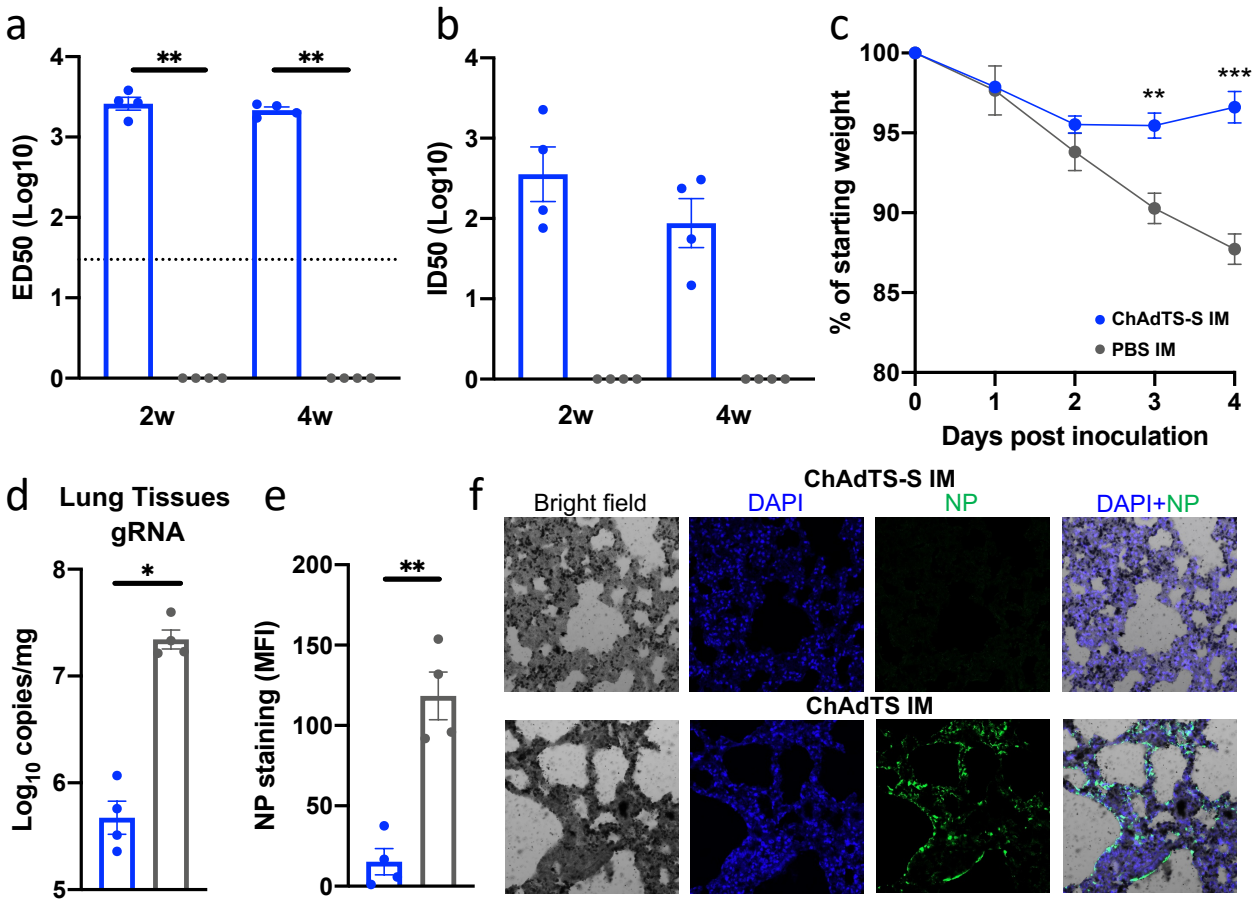
a
ED50 (Log10)
**
**
2w
4w
b
ID50 (Log10)
2w
4w
c
% of starting weight
**
***
ChAdTS-S IM
PBS IM
Days post inoculation
d
Lung Tissues
gRNA
Log10 copies/mg
*
e
NP staining (MFI)
**
f
ChAdTS-S IM
Bright field
DAPI
NP
DAPI+NP
ChAdTS IM

Fig.6

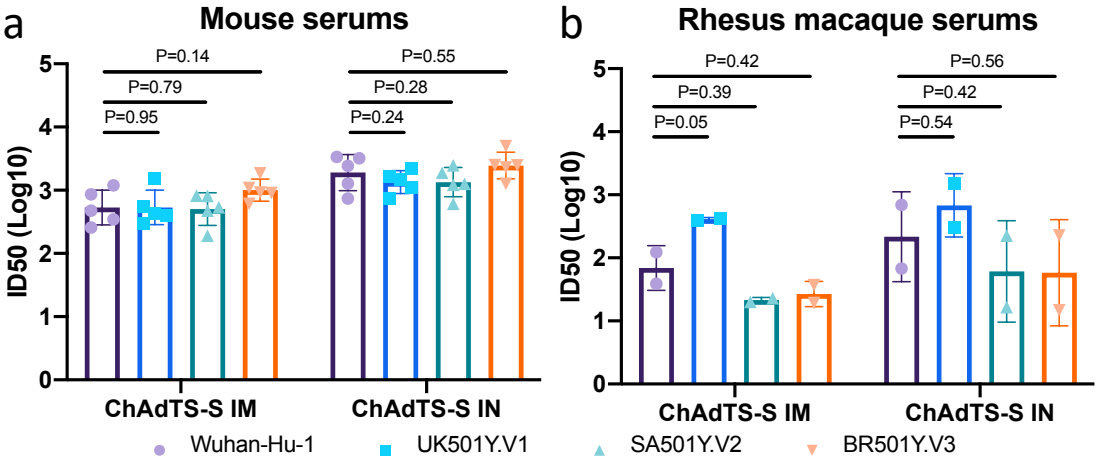
a
Mouse serums
P=0.14
P=0.79
P=0.95
P=0.55
P=0.28
P=0.24
ID50 (Log10)
0
1
2
3
4
5
ChAdTS-S IM
ChAdTS-S IN
Wuhan-Hu-1
UK501Y.V1
SA501Y.V2
BR501Y.V3
b
Rhesus macaque serums
P=0.42
P=0.39
P=0.05
P=0.56
P=0.42
P=0.54
ID50 (Log10)
0
1
2
3
4
5
ChAdTS-S IM
ChAdTS-S IN

Figures

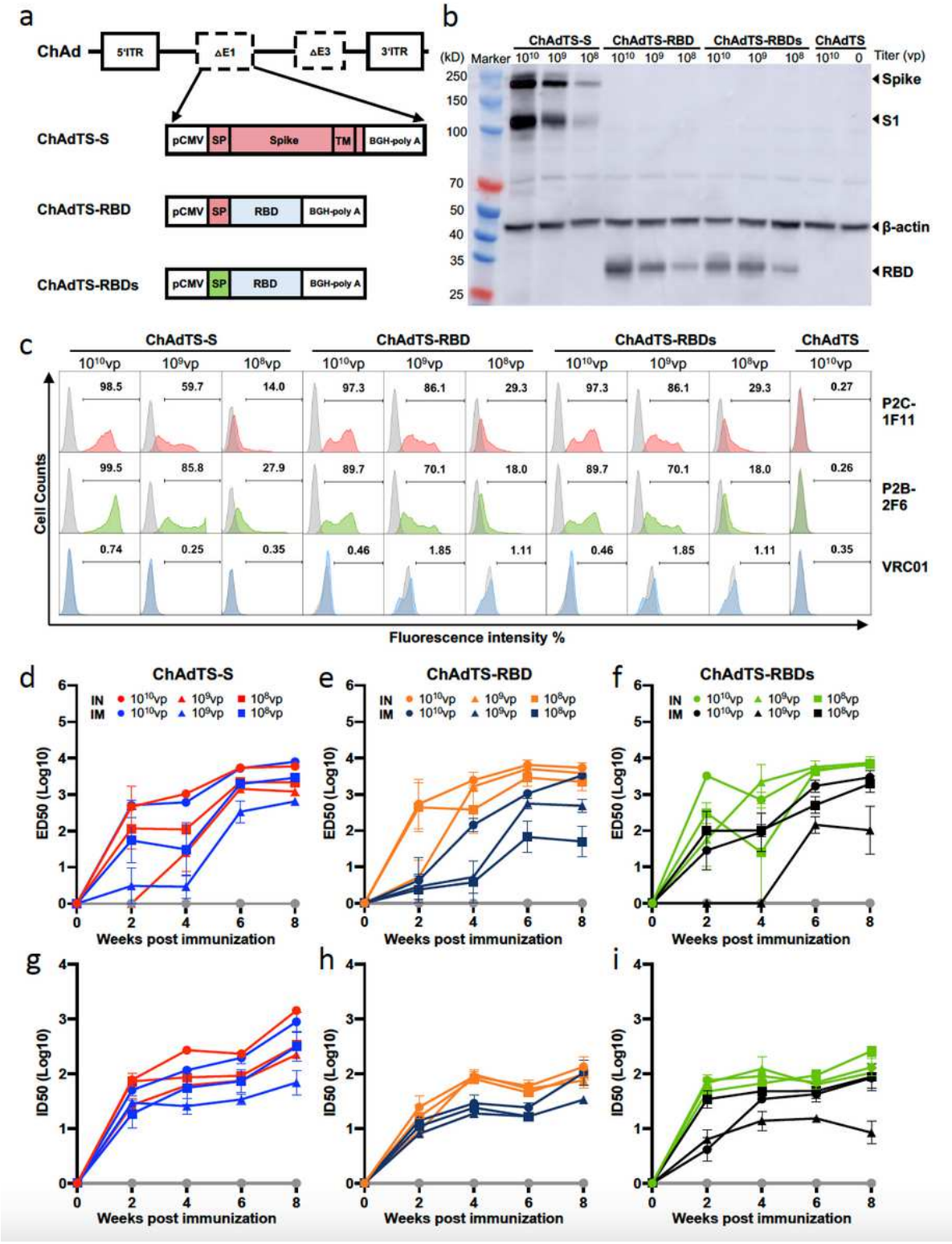

Figure 1

Generation and characterization of recombinant ChAdTS expressing the full-length spike protein or RBD of SARS-CoV-2. (a) Schematic diagram of the recombinant ChAdTS expressing the full-length S protein with its original signal peptide (ChAdTS-S), RBD with the original signal peptide from the S protein

(ChAdTSRBD), or RBD with the secretory signal peptide from mouse IgG (ChAdTS-RBDs). The coding sequence of the S protein or RBD was inserted into the E1 region of the ChAdTS vector under the control of the CMV promoter and terminated using a bovine growth hormone (BGH) polyadenylation signal sequence. (b) Western blot analysis of S and RBD expression in HEK293T cells infected with the recombinant ChAdTS (108, 109 and 1010 vp). (c) Flow cytometry analysis of S and RBD expression using the SARS-CoV-2-specific mAbs P2C-1F11 and P2B-2F6. HEK293T cell lysates and intact HEK293T cells infected with the empty ChAdTS vector (1010 vp) were used as negative controls. VRC01 was used as a negative control antibody. Serum binding activity to SARS-CoV-2 RBD (d, e, f) and neutralizing activity against pseudotyped SARS-CoV-2 (g, h, i) over an 8-week period after single-dose immunization with ChAdTS-S, ChAdTS-RBD or ChAdTS-RBDs. For each recombinant ChAdTS construct, three different doses (1010, 109, and 108 vp) were administered through either the intranasal (IN) or intramuscular (IM) route, which is indicated by different symbols and colors. Data points corresponding to animals in the empty ChAdTS vector control groups (1010 vp) are shown in grey. All data are presented as means ± SEM.

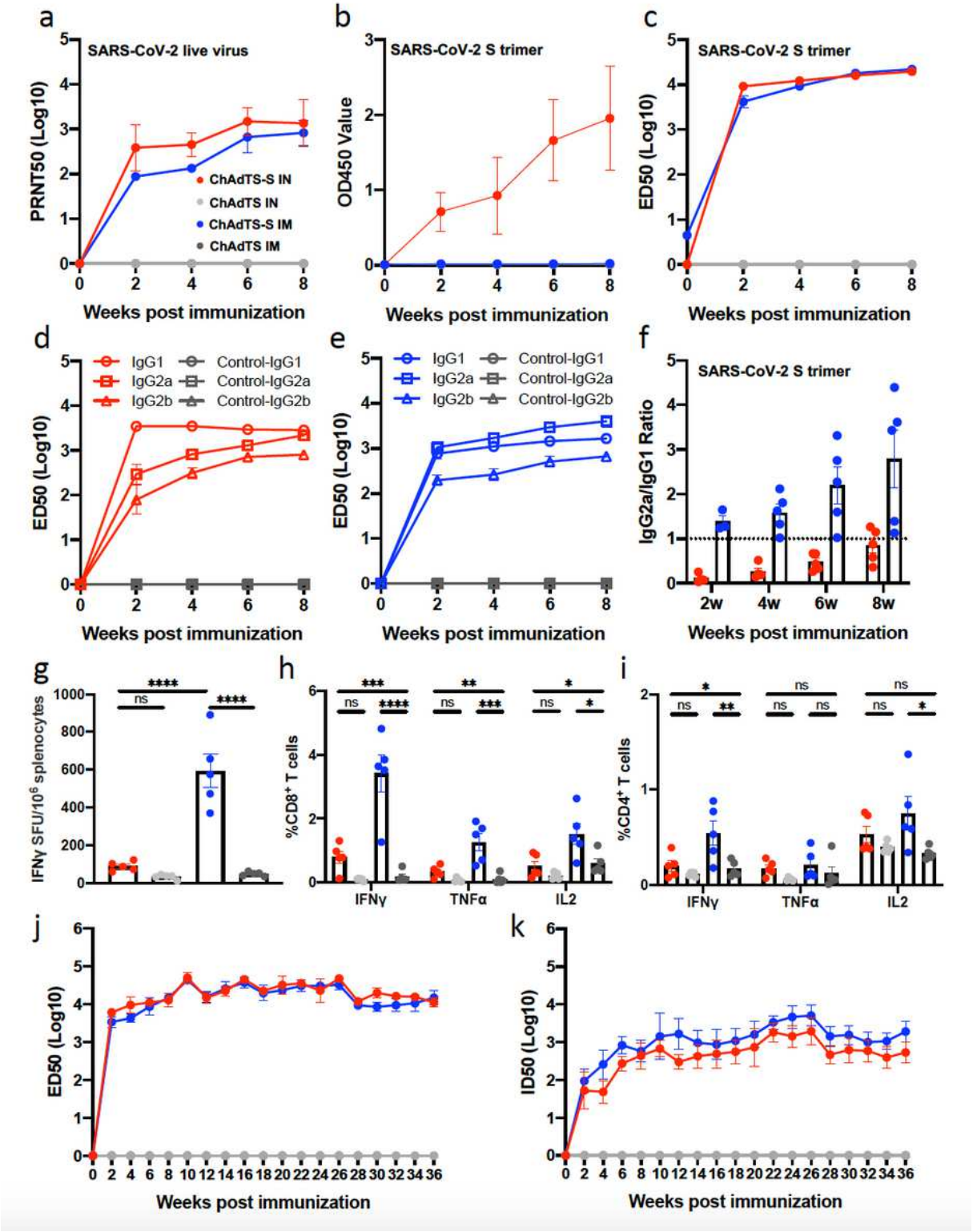

Figure 2

ChAdTS-S induces strong and durable immune responses in BALB/c mice. Animals immunized with 1010 vp of ChAdTS-S were characterized in greater detail. (a) Neutralizing activity of the immunized serum against live SARS-CoV-2 over an 8-week period after immunization. (b) Binding activity of total saliva IgA and (c) immune serum total IgG with the SARS-CoV-2 S trimer. Binding activity of immune serum IgG subtypes IgG1, IgG2a, and IgG2b with the SARS-CoV-2 S trimer in the (d) IN or (e) IM group. (f) The

IgG2a/IgG1 ratios in the IN and IM groups. (g) ELISPOT analysis for IFN-γ-positive splenocytes and FACS analysis of intracellular IFN-γ, TNF- α, and IL-2 production in (h) CD8+ and (i) CD4+ splenic T cells two weeks after immunization. The durability of the antibody response was analyzed using (j) ELISA with the SARS-CoV-2 S trimer and (k) pseudovirus neutralization up to 36 weeks after single-dose immunization. Data corresponding to animals in the IN group are shown in red, those in the IM group in blue, and those in the control group in grey. All data are presented as the means ± SEM. Analysis of unpaired Students' t-test (two-tailed) was used to determine the statistical significance of differences among different groups (*P < 0.05; **P < 0.01; ***P < 0.001; ****P < 0.0001; n.s., not significant).

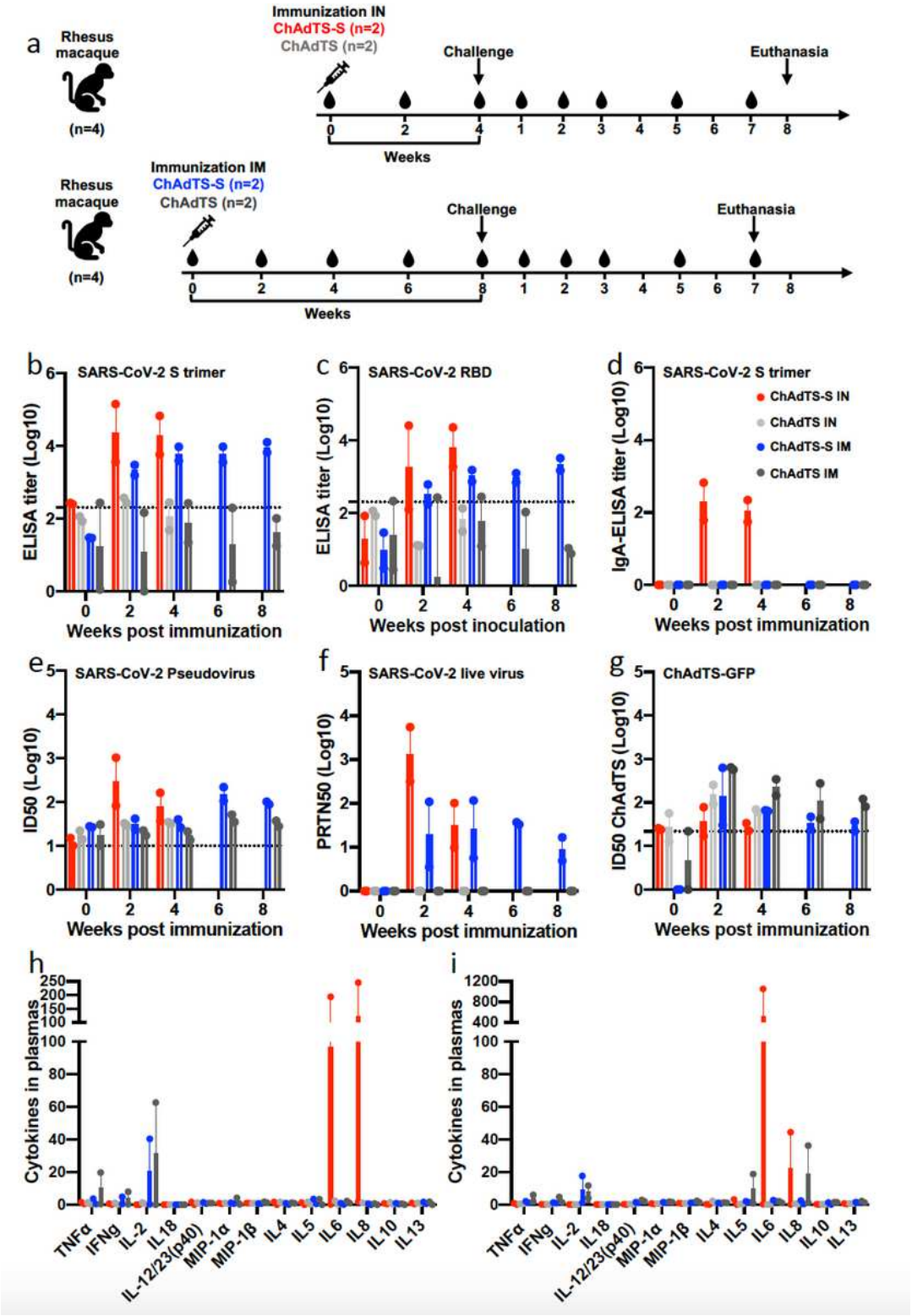

Figure 3

ChAdTS-S induces strong immune responses in rhesus macaques. (a) Timeline for vaccination followed by virological and immunological characterization in two groups of animals. In group one, four animals were intranasally immunized with 1011 vp of ChAdTS-S (n=2) or 1011 vp of the empty ChAdTS vector (n=2). After 4 weeks post-immunization, the animals were challenged with 106 PFU of live SARS-CoV-2. In group two, the same protocol was followed except that immunization was conducted via the IM route and

challenge was carried out 8 weeks after immunization. Blood samples were collected every 2 weeks before viral challenge. Blood samples and nasal swabs were also collected on days 0, 1, 2, 3, 5, and 7 after the challenge. All animals were euthanized on day 7 or 8 after the challenge to quantify the viral load in the lung tissue and conduct histopathological examinations. Binding activity of immune serum total IgG with the SARS-CoV-2 S trimer (b), SARS-CoV-2 RBD (c), or total IgA with the SARS-CoV-2 S trimer (d). Neutralizing activity of immunized serum against pseudovirus (e) and live SARS-CoV-2 (f). Neutralizing activity of immunized serum against the empty ChAdTS vector was assessed using a ChAdTS-GFP neutralization assay (g). Serum levels of cytokines were measured on week 2 (h) and week 4 (i) after immunization. Data corresponding to animals in the IN group are shown in red, those in the IM group in blue, and those in the control group in grey. All data are presented as the means ± SEM.

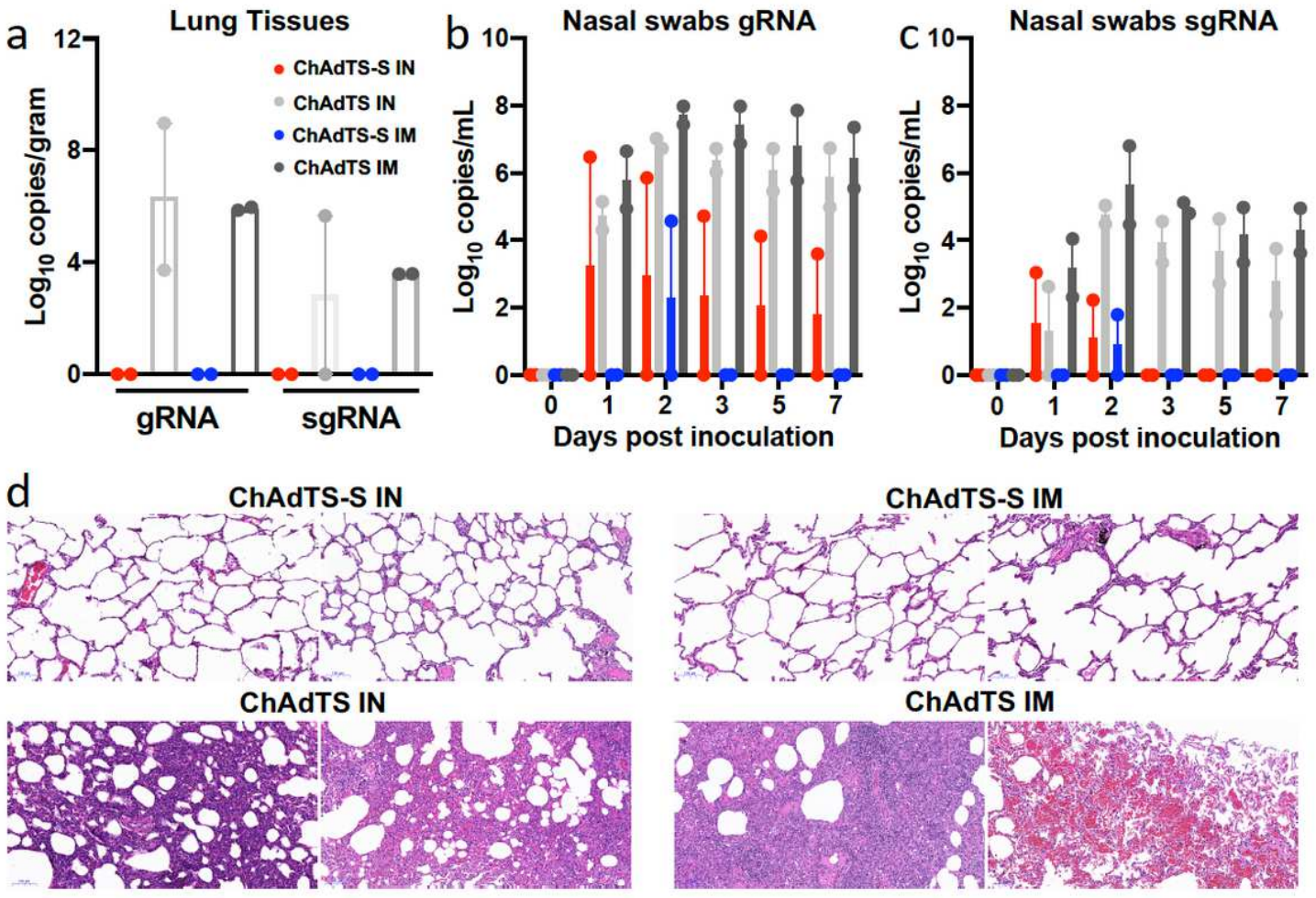

Figure 4

Vaccination with ChAdTS-S elicits a protective immune response against SARS-CoV-2 infection in rhesus macaques. (a) The total number of viral gRNA and sgRNA copies in lung tissue samples from six lobes was quantified by droplet digital PCR (TargetingOne, China). (b) Viral gRNA and (c) sgRNA in the nasal swabs were monitored and quantified using the same technique up to day 7 after viral challenge. (d) Histopathological comparison of tissues from animals vaccinated with ChAdTS-S and the empty ChAdTS vector animals. Representative tissue sections in standard hematoxylin and eosin staining are

shown (10×). The scale bar is 100 μm. Data corresponding to animals in the IN group are shown in red, those in the IM group in blue, and those in the control group in grey. All data are presented as means ± SEM.

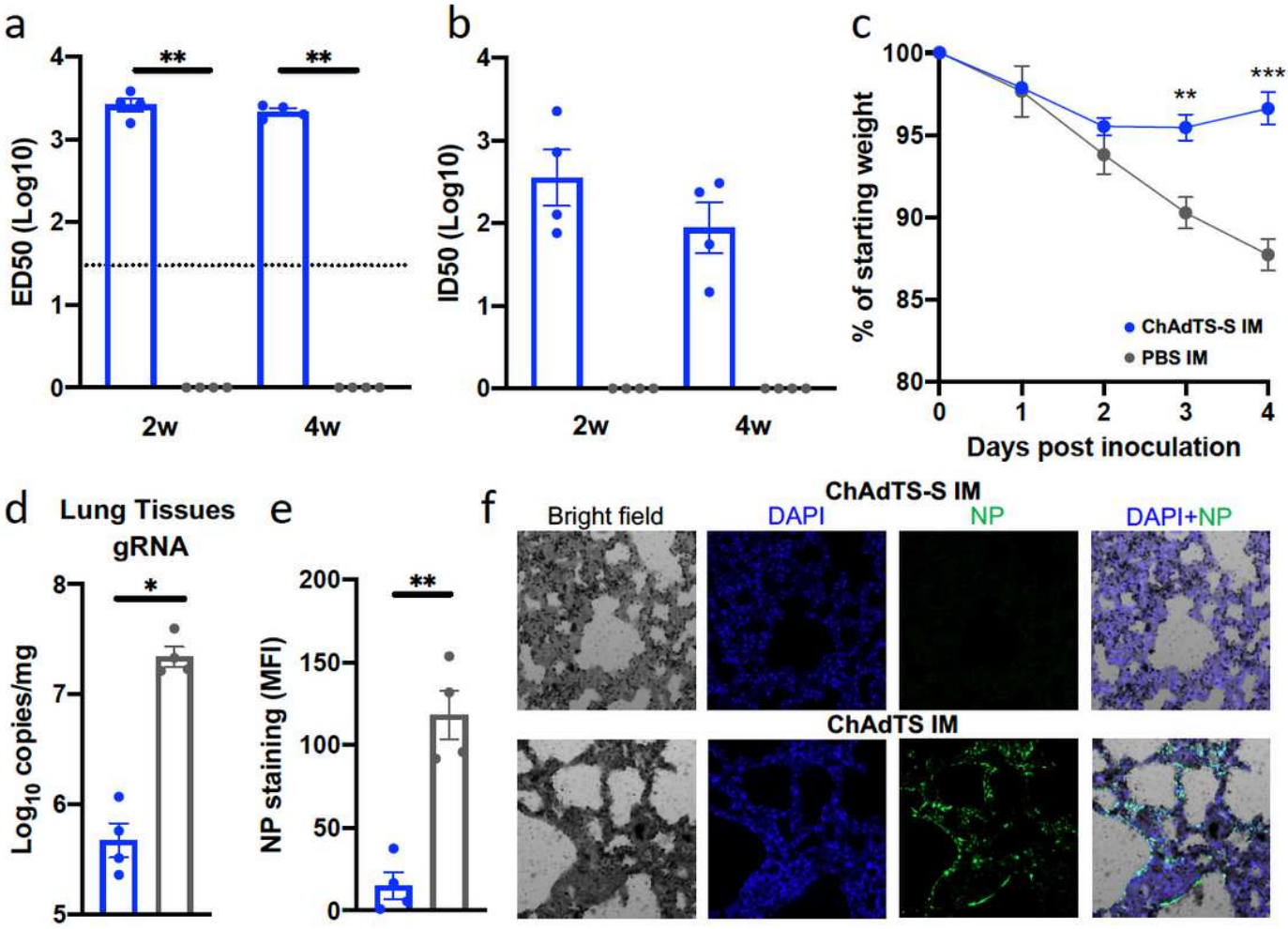

Figure 5

Vaccination with ChAdTS-S elicits a protective immune response against SARS-CoV-2 infection in golden Syrian hamsters. The hamsters were immunized with ChAdTS-S (n=4) or saline as control (n=4) via the IM route. (a) The binding ability of the immunized serum for SARS-CoV-2 RBD on week 2 and week 4 after immunization was assessed. (b) The neutralizing ability of the serum against SARS-CoV-2 pseudovirus. Intranasal challenge with 105 plaque-forming units (PFU) of the HKU-13 strain of SARS-CoV-2 was carried out at 6 weeks post immunization. (c) Weight loss in SARS-CoV-2 challenged hamsters. Four days after the challenge, lung tissues were harvested to quantify the viral load using qPCR (d) and by immunostaining lung tissue sections using a specific monoclonal antibody against SARS-CoV-2 nucleocapsid protein (20×) (e,f). Data corresponding to animals in the IM group in blue, and those in the control group in grey. All data are presented as the means ± SEM. Analysis of unpaired Students' t-test (two-tailed) was used (*P < 0.05; **P < 0.01; ***P < 0.001).

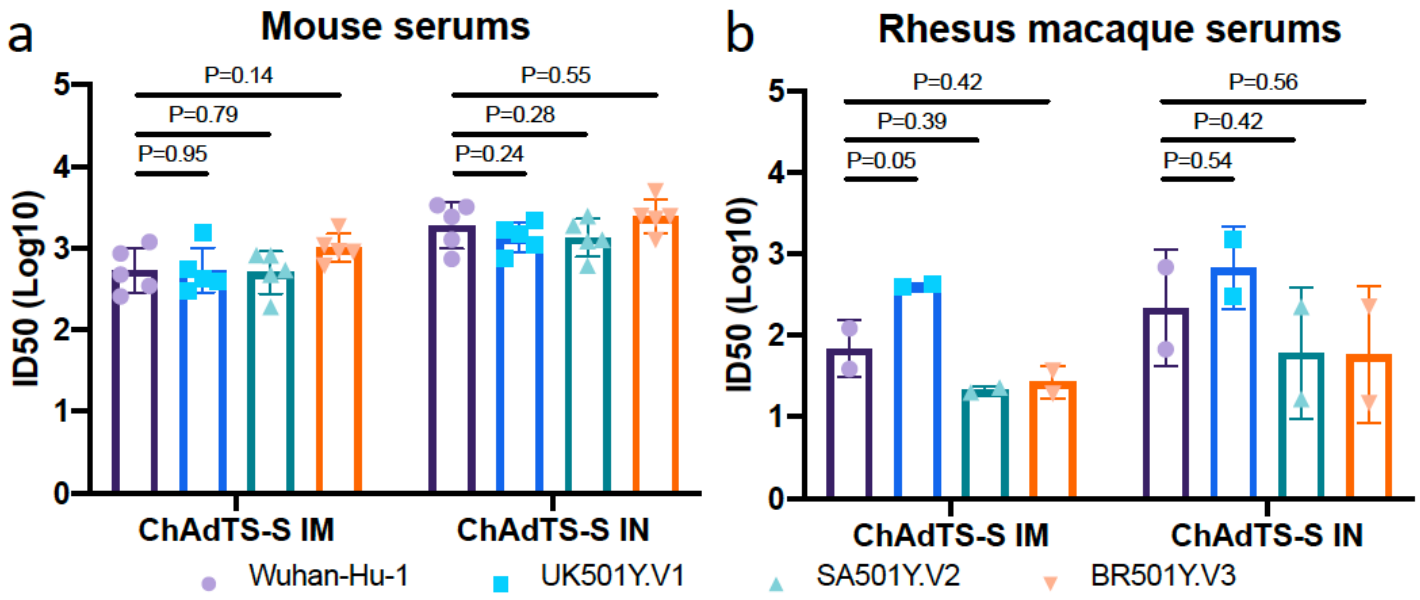

Figure 6

Neutralization titers of immune sera from vaccinated BALB/c mice and rhesus macaques against wildtype and new variants of SARS-CoV-2. Sera samples were collected and analyzed against pseudoviruses carrying S protein either from wildtype Wuhan-Hu-1, UK501Y.V1, SA501Y.V2 or BR501Y.V3. (a) Neutralizing activity of immune sera from BALB/c mice 36 weeks post immunization and (b) from rhesus macaques 2 weeks post IN immunization and 6 weeks post IM immunization. All data are presented as the means ± SEM. Analysis of unpaired Students' t-test (twotailed) was used.